

Master Thesis in Machine Elements

---

# **Transmission Modeling for Optimization of Electric Powertrains**

---

Johanna Hulth Olsson  
Jacob Lundborg

June 14, 2021

Department of Machine Elements  
Faculty of Engineering  
Lund University  
Lund, Sweden

Supervisors:

Rikard Hjelm, Department of Machine Elements  
Henrik Nilsson, BorgWarner Sweden AB in Landskrona, Sweden

Examiner:

Professor Jens Wahlström, Department of Machine Elements

© 2021 by Johanna Hulth Olsson and Jacob Lundborg. All rights reserved.

ISRN: LUTMDN/TMME-5007-SE

# Abstract

Over the last decade, the number of electric vehicles (EVs) on the world's roads has rapidly increased. Optimization of power consumption in electric powertrains will, therefore, lead to reduced energy usage in the road transport sector. EPOS, is a research project that aims to optimize EV powertrains, with the objectives to minimize cost and power consumption. As a part of the EPOS project, this thesis' purpose was to develop an optimization tool for the mechanical transmissions in EVs, with the objectives to minimize mass and power loss. The optimization tool is intended to run millions of times, therefore a target for execution time for the transmission optimizations was set. Models for component size and efficiency were initially created with a high level of detail, which was subsequently reduced in order to reach the target for execution time. Fixed values for design variables and an iteration based gear-set optimization model lead to successfully reaching the target, but solutions were less optimized. The fixed variables' impact on the optimization result could be evaluated, by comparing the optimization solutions while varying the number of fixed design variables. The optimal solution was determined with a scoring model, that compared the optimization objectives in terms of energy consumption. It was found that there was a significant trade-off when minimizing mass and power loss. Prioritization in the trade-off was important when deciding on an optimal solution, in order to get the desired result. The final conclusion of this thesis was that the detail of component models and the compromise between optimization objectives, have an important role in attaining the most optimal transmission design.

# Acknowledgments

This master thesis was performed at the Department of Machine Elements, at the Faculty of Engineering of Lund University. The thesis was done in collaboration with BorgWarner. The thesis covers 30 credits and lasted from January to June of 2021.

A special thank you to Rikard Hjelm, for your guidance and support through out this whole project. Thanks to Henrik Nilsson, for your trust and every weekly meeting to support our work. Another thanks to Bradley Read at BorgWarner, for providing us with your expertise regarding gear design and transmission layouts. Thank you to those at BorgWarner who gave us valuable inputs and comments throughout this project. We would also like to thank everyone in the EPOS project, and especially thanks to Gabriel Domingues-Olavarria for all your help. Last but not least, we would like to thank our examiner, Professor Jens Wahlström and our opponents, Driton Sabani and Isa Yenibayrak. All your comments were of high value to us.

# Contents

<b>1</b>	<b>Introduction</b>	<b>1</b>
1.1	Background . . . . .	1
1.1.1	Electric powertrains . . . . .	1
1.1.2	The EPOS project . . . . .	2
1.2	Problem description . . . . .	3
1.3	Objectives . . . . .	4
1.4	Limitations . . . . .	4
<b>2</b>	<b>Methodology</b>	<b>5</b>
2.1	Program structure . . . . .	5
2.2	Layout models . . . . .	6
2.2.1	Layshaft models . . . . .	6
2.2.2	Multi-speed layshaft models . . . . .	8
2.2.3	Partial gear ratios of layshaft transmissions . . . . .	8
2.2.4	Gear mesh frequency . . . . .	9
2.3	Gear sizing model . . . . .	9
2.3.1	Contact stress limitation . . . . .	10
2.3.2	Bending stress limitation . . . . .	10
2.3.3	Constraints for gears . . . . .	11
2.4	Models for sizing of other components . . . . .	12
2.4.1	Shaft sizing model . . . . .	12
2.4.2	Bearing sizing model . . . . .	12
2.4.3	Auxiliary component models . . . . .	12
2.4.4	Packaging models . . . . .	13
2.5	Component efficiency models . . . . .	15
2.5.1	Load dependent losses . . . . .	15
2.5.2	Non-load dependent losses . . . . .	16
2.6	Scoring model . . . . .	17
2.7	Optimization process . . . . .	18
2.7.1	Gear-set optimization . . . . .	18
2.7.2	System optimization . . . . .	21
2.8	Model verification . . . . .	22
2.9	Model evaluation . . . . .	22
2.9.1	Testing execution time . . . . .	23
2.9.2	Evaluating the impact of fixed design variables . . . . .	23
<b>3</b>	<b>Results</b>	<b>24</b>
3.1	Execution time . . . . .	24
3.2	Fixed values of design variables . . . . .	27
3.2.1	Fixed value for helix angle . . . . .	27
3.2.2	Fixed values for profile shift coefficients . . . . .	28
3.2.3	Fixed value for pressure angle . . . . .	29
3.2.4	Fixed value for helix angle, profile shift coefficients, and pressure angle . . . . .	30
3.3	Trade-off between optimization objectives . . . . .	31
3.4	Running the finished transmission optimization tool . . . . .	32
<b>4</b>	<b>Discussion</b>	<b>38</b>
4.1	Evaluation of results . . . . .	38
4.2	Discussing the scoring model . . . . .	39
4.2.1	Mass' impact on power consumption . . . . .	39

4.2.2	Trade-off in reference literature . . . . .	39
4.2.3	Weighting of objectives . . . . .	39
4.2.4	Volume as a scoring objectives . . . . .	40
4.3	Optimization methods . . . . .	41
4.3.1	Gear-set optimization . . . . .	41
4.3.2	System optimization . . . . .	42
4.3.3	Alternative method for optimization . . . . .	43
4.4	MATLAB . . . . .	43
4.5	Sizing and efficiency models . . . . .	44
4.5.1	Gear sizing model . . . . .	44
4.5.2	Comparison of oil seal loss equations . . . . .	44
4.5.3	Model validation . . . . .	44
4.6	Objectives and limitations . . . . .	44
4.7	Further work . . . . .	45
4.7.1	System dynamics . . . . .	45
4.7.2	Detailed analysis of fixed values for design variables . . . . .	45
4.7.3	Planetary transmissions . . . . .	45
<b>5</b>	<b>Conclusion</b>	<b>47</b>
<b>A</b>	<b>Appendix</b>	<b>50</b>
A.1	Parameter values . . . . .	50
A.2	Comparison for verification data . . . . .	51
A.3	Visual evaluation of trends in population data . . . . .	52

# List of Figures

1.1	Global stock of electric cars. Figure adapted from IEA [1]. . . . .	1
1.2	The three parts of the EV powertrain. The black outline indicates the focus of this thesis. . . . .	2
1.3	Black box representation of the transmission optimization tool. . . . .	3
2.1	Method for development of the transmission optimization tool. . . . .	5
2.2	Two-stage layshaft layout. . . . .	7
2.3	Structure of the two-stage layshaft layout model in the transmission optimization tool. . . . .	7
2.4	Multi-speed two-stage layshaft layout. . . . .	8
2.5	Rim thickness and tooth height of a gear. . . . .	11
2.6	Outer dimensions of a two stage layshaft model. . . . .	13
2.7	Outer dimensions of a three stage layshaft model. . . . .	14
2.8	Process for gear-set optimization. . . . .	19
2.9	Iteration process of a simplified gear-set optimization, corresponding to the example. . . . .	20
2.10	Visual representation of solutions calculated by using iteration based optimization. . . . .	21
2.11	Population of the system optimization. . . . .	22
3.1	Execution time of "Case 0". The horizontal lines are mean values of the execution time, for the respective speeds. . . . .	24
3.2	Execution time of "Case 1". The horizontal lines are mean values of the execution time, for the respective speeds. . . . .	24
3.3	Execution time of "Case 2". The horizontal lines are mean values of the execution time, for the respective speeds. . . . .	25
3.4	Execution time of "Case 3". The horizontal lines are mean values of the execution time, for the respective speeds. . . . .	25
3.5	Execution time of "Case 4". The horizontal lines are mean values of the execution time, for the respective speeds. . . . .	26
3.6	Increase in system power loss (left) and mass (right) when using a fixed value for helix angle instead of letting the optimizer find optimal values for helix angle. . . . .	27
3.7	Increase in system power loss (left) and mass (right) when using fixed value for profile shift coefficients instead of letting the gear optimizer find optimal values. . . . .	28
3.8	Increase in system power loss (left) and mass (right) when using fixed value for the pressure angle instead of letting the gear optimizer find optimal values. . . . .	29
3.9	Increase in system power loss (left) and mass (right) when using fixed values for helix angle, profile shift coefficients, and pressure angle, instead of optimizing them. . . . .	30
3.10	Mass and efficiency of system solutions. The trade-off between the objectives is clearly visualized by the plotted curve. . . . .	31
3.11	Graphical representation of efficiency map of the two-stage single-speed transmission, with input data from Table 3.1. . . . .	32
3.12	Visual result of modeling optimization tool output parameters in MASTA, with input data from Table 3.1. . . . .	34
3.13	Graphical representation of efficiency map of the two-stage two-speed transmission, with input data from Table 3.3. . . . .	35
3.14	Visual result of modeling optimization tool output parameters in MASTA. A two-speed two-stage layshaft transmission defined by parameters in Table 3.3. . . . .	37
4.1	Transmission systems with the same input parameters, but with different weighting factor for objectives, according to Table 4.1 . . . . .	40
4.2	Determination of top solution of a data set, dependent on distance between sample points, $L_{step}$ . The colored bars represent the sampling points. . . . .	42
A.1	Plots of sample data for visual analysis of trends depending on input torque. Shows the difference in system power loss (top) and system mass (bottom) depending on torque. . . . .	52

A.2	Plots of sample data for visual analysis of trends depending on gear ratio. Shows the difference in system power loss (top) and system mass (bottom) depending on gear ratio. . . . .	53
-----	---	----



# List of Tables

2.1	The optimization tool's different models. . . . .	6
2.2	The power loss equations used for component models. . . . .	15
2.3	Parameters and parameter values for estimation on the mass' effect on the power consumption, in the example in Equation 34. . . . .	17
2.4	Variable and constant design parameters for gear design. . . . .	18
2.5	Cases used for testing the transmission optimization tool for a single-speed two-stage layshaft transmission. . . . .	22
3.1	Input parameter values for testing transmission optimization tool for a two-speed two-stage layshaft transmission. . . . .	32
3.2	Output values from testing transmission optimization tool for a single-speed two-stage layshaft transmission. . . . .	33
3.3	Input parameter values for testing transmission optimization tool for a two-speed two-stage layshaft transmission. . . . .	35
3.4	Output values from testing transmission optimization tool for a two-speed two-stage layshaft . . . . .	36
4.1	Data for transmission systems in Figure 4.1. . . . .	40
4.2	Transmission mass and efficiency of optimal solutions depending on excluding or including the transmission's volume in the scoring model (input data from Table 3.1). . . . .	41
4.3	Number of iterations for gear mesh optimization, and how it affects execution time and deviation from the score when using one iteration. . . . .	42
4.4	Seal power loss equations considered in this thesis. . . . .	44
A.1	Summary of factors for sizing of involute gears according to ISO 6336 [18]. Factors without a specified value are calculated in the models. . . . .	50
A.2	Comparison between transmission optimization tool output and MASTA. . . . .	51

# Nomenclature

Symbol	Name	Unit
$\alpha_n$	Normal pressure angle	$^\circ$
$\beta$	Helix angle	$^\circ$
$\eta_m$	Factor for mass power loss	—
$\eta_P$	System efficiency for power loss	—
$\gamma$	Diversion angle	$^\circ$
$\nu$	Kinematic viscosity	$mm^2/s$
$\rho$	Density	$kg/mm^3$
$\sigma_F$	Tooth root stress	$N/mm^2$
$\sigma_H$	Contact stress	$N/mm^2$
$\theta$	Operating temperature of the oil	$^\circ C$
$a$	Center distance	$mm$
$b$	Face width ( $= b_0 m_n$ )	$mm$
$b_0$	Coefficient of face width	—
$d$	Reference diameter	$mm$
$d_{sh}$	Shaft diameter	$mm$
$F_t$	Transverse tangential load on reference cylinder	$N$
$GMF$	Gear mesh frequency	$Hz$
$H$	Approximated height of transmission	$mm$
$K$	Factors for gear mesh load (Table A.1, p. 51)	—
$L$	Approximated length of transmission	$mm$
$m$	Mass	$kg$
$m_n$	Normal module	$mm$
$M_{totN}$	Total mass of an N-stage transmission	—
$n$	Rotational velocity	$rpm$
$P_M$	Gear mesh power loss	$kW$
$P_{BW}$	Bearing churning and windage power loss	$kW$
$P_B$	Bearing loaded power loss	$kW$
$P_{GW}$	Gear churning and windage power loss	$kW$
$P_{in}$	Input power from the motor	$kW$
$P_{loss}$	Total power loss from all the components	$kW$
$P_{VD}$	Oil seal power loss	$kW$
$s$	Component clearance	$mm$
$S_F$	Safety factor for tooth bending	—
$S_H$	Safety factor for pitting	—

$T$	Torque	$Nm$
$t$	Wall thickness of transmission housing	$mm$
$U$	Total gear ratio	–
$u$	Partial gear ratio for a gear stage	–
$V$	Approximated volume of transmission	$mm^3$
$W$	Approximated width of transmission	$mm$
$x_0$	Profile shift coefficient	–
$Y$	Factors related to tooth bending (Table A.1, p. 51)	–
$Z$	Factors related to contact stress (Table A.1, p. 51)	–
$z$	Number of teeth	–

# 1 Introduction

## 1.1 Background

From the year 2010, the amount of electric vehicles (EVs) on the world's roads has increased from 17 thousand to above 10 million, according to the International Energy Agency (IEA) [1]. One factor behind the increase in EV sales is the environmental sustainability objectives, which EVs can fulfill by reducing tailpipe emissions from road transport [2]. The transport sector accounts for 24% of global  $CO_2$  emissions, of which three quarters are associated with road transport [3].

As seen in Figure 1.1 the global EV stock has rapidly increased since the beginning of the last decade. In 2019, EV sales accounted for 2.6% of global car sales, which raised the stock to 1% of the global car fleet [3].

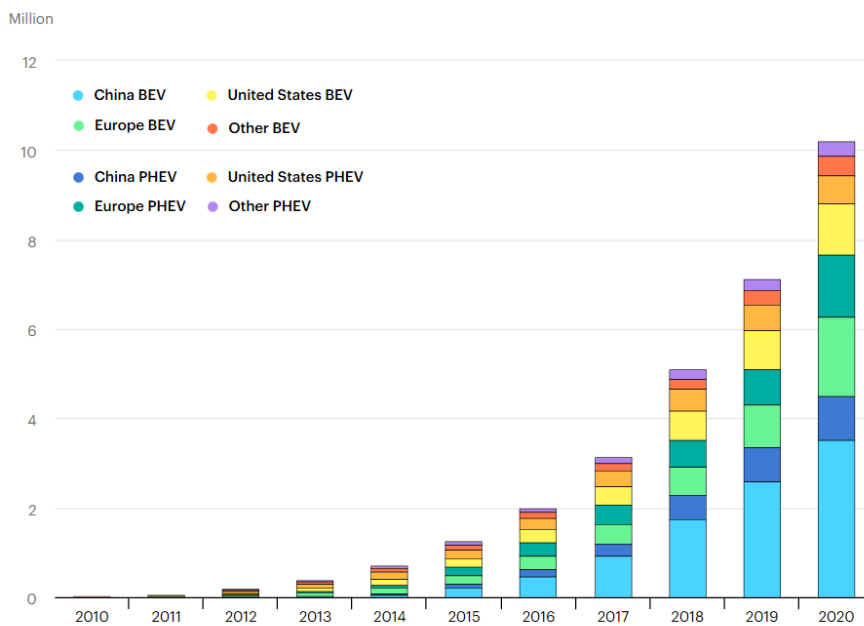


**Figure 1.1:** Global stock of electric cars. Figure adapted from IEA [1].

Electric vehicles are undeniably taking a substantial role in the future of mobility, and have potential to reduce carbon emissions in the transport sector. According to IEA [2], most of EVs' greenhouse gas emissions are from the use phase. Thus, there is a great incentive to increase the efficiency of the electric powertrain, in order to lower the overall emissions. The importance of optimizing efficiency of electric powertrains is further strengthened as sustainability interests in industry increases, and as Michaelis et al. [4] put it: "future energy shortages have to be fought not only with exploitation of new renewable energy resources but also with reduction of energy consumption in all technical fields".

### 1.1.1 Electric powertrains

The powertrain of electric vehicles can be divided in three parts: power electronic converter (PEC), electrical machines (EMs), and mechanical transmissions (MTs). In Figure 1.2 a simplified EV powertrain is illustrated.

The EV's source of propulsion is the electric motor. The EM has the ability to convert electrical energy to rotational energy, thus supplying the vehicle's wheels with torque. In order to ensure

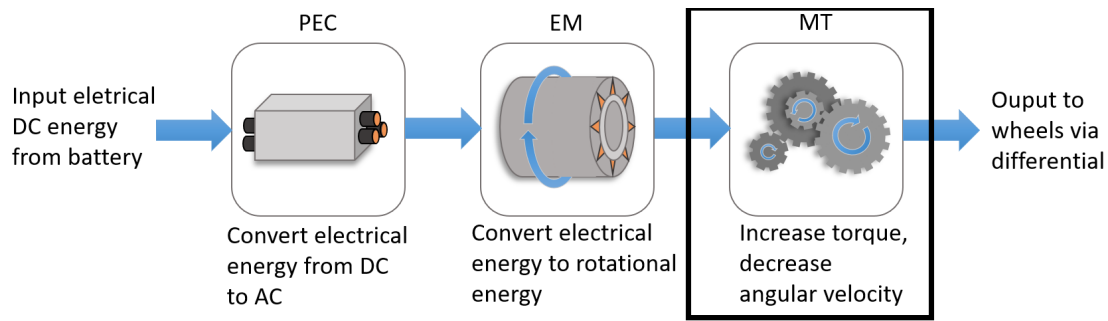


**Figure 1.2:** The three parts of the EV powertrain. The black outline indicates the focus of this thesis.

the correct torque and rotational velocity of the EM, the PEC controls the EM by regulating the input power [5].

It is beneficial for the EM to operate at lower torques and higher speeds than the desired output to the wheels [5]. Instead of increasing the size of the EM, the desired output torque can be met by connecting the motor to a mechanical transmission. If torque is increased via the gear ratio, the rotational speed from the motor is decreased by roughly the same ratio.

Domingues-Olavarria et al. [6] present a methodology for modeling the components of the electric powertrain to find an optimal preliminary system design, in order to minimize mass and cost with a wide variety of constraints. The proposed methodology allows EV manufacturers to find a suitable powertrain design for a specific electromobility application. According to Domingues-Olavarria et al. [6], most studies of optimizing electric powertrains pay less attention to the mechanical transmissions' impact, compared to the electric components'. But transmission modeling and optimization is certainly done in other fields of research [7, 8, 9].

### 1.1.2 The EPOS project

EPOS (Electric Powertrain Optimization for Vehicles and Fleets) is an ongoing research project in the field of electromobility. EPOS is a collaboration project between Lund University, Borg-Warner, and Haldex, with sponsorship from the Swedish Energy Agency.

The objective of the entire EPOS project is to develop an optimization tool for electric powertrains, regarding minimizing cost and/or energy consumption. Previous studies in the EPOS project have primarily been focused on electric motors and power electronics, using only simple transmission models [10, 11], which has resulted in a research gap in optimization of mechanical transmissions. The simple transmission models previously used consisted of sizing of gears and shafts, while bearings and component efficiency were not modeled.

EPOS' optimization process is based on comparisons between millions of simulated powertrains with unique transmissions. The transmission optimization tool needs to produce an optimal solution in relatively short amount of time, since otherwise the whole simulation will become too time consuming. Therefore, there is an objective to keep down execution time for the transmission optimization.

One application of the electric powertrain optimization tool is to study the impact of having mechanical transmissions with several different speeds, and how it affects the powertrain's overall performance. With a multi-speed transmission, vehicles can achieve both high acceleration at low speeds and a high top speed [12].

A multi-speed transmission contains multiple gear-sets with different gear ratios, which allows the EM to work in the higher efficiency regions during more time of the drive cycle [13]. The number of speeds, e.g. two, three, or four, are dependent on the desired operating points of the

EM. The use of more gears will improve overall efficiency of the EM, but a higher number of gears affects manufacturing cost, packaging constraints, and reliability of the gearbox [14].

## 1.2 Problem description

The motive of this master thesis is to fill the current research gap in optimization of transmission models, which is required to fulfill the EPOS project's objective to create an optimization tool for the entire electric powertrain. The part of the electric powertrain covered by this thesis is marked with a black outline in Figure 1.2.

As mentioned in Section 1.1.2 "The EPOS project", the main objectives of the optimization tool are to minimize cost and energy consumption of the electric powertrain. However, the mechanical transmissions modeled in this thesis are optimized for minimized mass and energy consumption. The implementation of a cost model for the mechanical transmissions is outside the scope of this thesis.

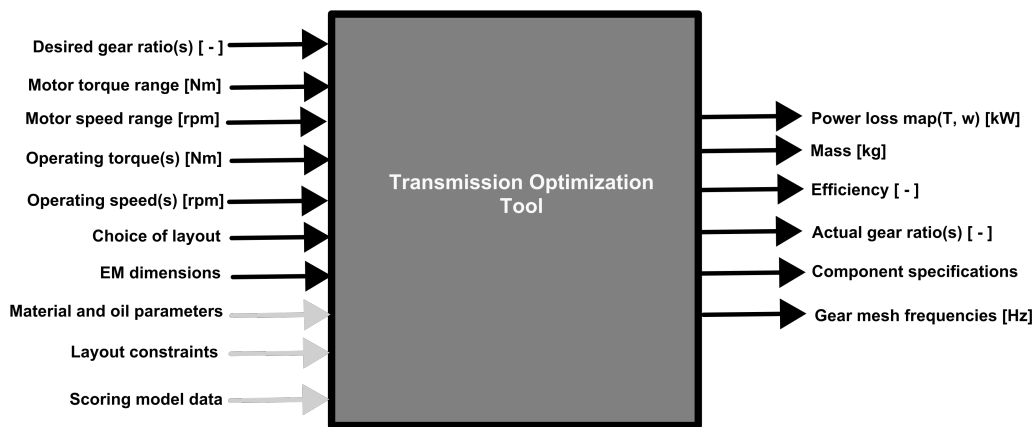


**Figure 1.3:** Black box representation of the transmission optimization tool.

Figure 1.3 illustrates the transmission optimization tool as a "black box", depicting all input and output parameters, some of which are clarified below.

- When optimizing a transmission a "layout" is chosen, and with it "layout constraints" are obtained.
- Material and oil parameters are set by the user. The material of gears can for instance be changed into powder metal.
- Operating torque and speed are specified for the desired gear ratio. If the transmission consists of several speeds, operating points are defined separately for each gear ratio. The operating points are used when determining the efficiency of the transmission system.
- Data for the scoring model are input, as the scoring model's result depends on the vehicle being optimized.
- Since the number of teeth are integers, and there are certain constraints for which teeth combinations are allowed for meshing gears, there may not always be a transmission solution with the exact desirable gear ratio. Hence, the actual gear ratios are output from the model.
- Component specifications contains data for components, e.g. gear modules and bearing diameters.

Gear train optimization have been subject to many previous studies outside of electric powertrain optimization. For example, Kim et al. [7] researched the optimization of a helical gear set,

Patil et al. [8] investigated the optimization of a two-stage helical gearbox, and Mendi et al. [9] performed a similar investigation. Compared to the mentioned studies, this thesis has the objective of keeping down execution time, as it is part of an electric powertrain optimization tool developed in the EPOS project.

As mentioned in Section 1.1.2 "The EPOS project", the execution time of the transmission optimization tool was of high importance. Therefore, a target for the execution time of optimizing one transmission was set to 100 milliseconds (on a DELL laptop running Windows 10, with a 6 Core 2.70 GHz Intel Core i7 processor, and 16 GB of RAM). The prior transmission optimization in the EPOS project had an execution time of  $\sim 60$  ms, and since the optimization was supplemented with additional models the execution was allowed to increase slightly.

### 1.3 Objectives

The purpose of this master thesis was to develop models for optimizing the mechanical transmission system as a part of an electric powertrain optimization tool, to fill the research gap of the EPOS project. In order to fill the research gap, the main objective to fulfill was:

*RQ1: "How can a tool for optimizing the mechanical transmissions in EVs be designed, in order to minimize mass and power losses?"*

To achieve the main objective, modeling of components and their power losses was necessary. Further objectives were to increase system know-how and methodology for global optimization, and provide an answer to the question:

*RQ2: "Which trade-offs occur when optimizing the mechanical transmissions?"*

Since there was a target for execution time, there was a limit in how detailed the optimization could be. Therefore, a third research question was investigated.

*RQ3: "How does a limit in execution time influence the accuracy of the optimization result?"*

### 1.4 Limitations

This thesis was limited to describing and modeling mechanical transmissions of the powertrain of electric vehicles. The mechanical transmission is seen as the part of the powertrain that begins with the output shaft from the motor, and ends with the differential. Other parts of the powertrain (EMs and PEC) are not described more than in Section 1.1.1 "Electric powertrains". However, some motor specifications are used as inputs to the transmission optimization tool, as can be seen in Figure 1.3.

Limitations of this thesis were:

1. Cost of components were not considered.
2. A static load case was assumed for the transmission models.
3. Sizing and efficiency of the differential were not investigated. However, bearings on the differential were modeled.
4. Sizing and efficiency of shifting elements were not considered for multi-speed transmissions.
5. Only layshaft transmissions were modeled in this thesis.

## 2 Methodology

In order to achieve the optimal system optimization it would be necessary to vary every design parameters of all components at once, to cover the dependencies between components. Varying more parameters leads to a higher level of detail, but would result in a vast amount of calculations and long execution time. The transmission optimization in this thesis was developed with a high level of detail, which after evaluation could be reduced in order to decrease execution time.

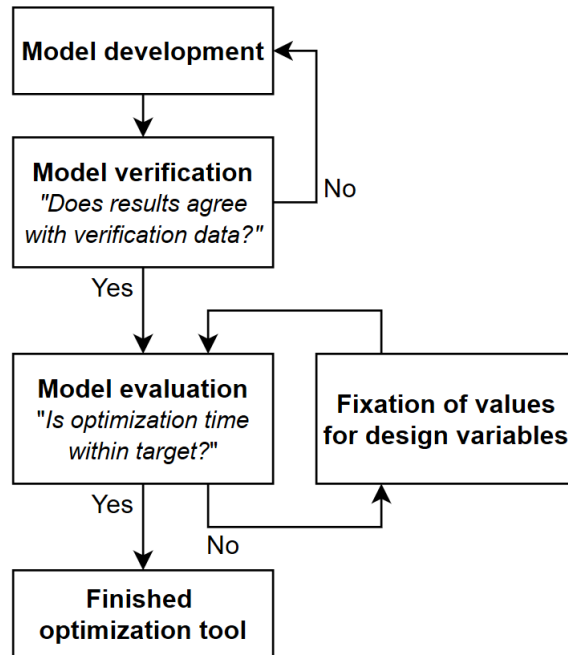


**Figure 2.1:** Method for development of the transmission optimization tool.

The steps in the development process in Figure 2.1 are described below.

**Model development** defined the process of creating all models that make up the optimization tool.

**Model verification** entailed the process of comparing the output data from the models with geometrical parameters, durability calculations, and efficiency results from a commercial software for gearbox and driveline design, analysis, and optimization.

**Model evaluation** was the process of measuring the execution time, and evaluating the influence of design variables and optimization strategies. The target for execution time needed to be met, if not, the models had to be adjusted in order to reach the target.

**Fixation of values for design variables** was done as a measure to decrease the execution time. After evaluation it was determined that certain design variables could be substituted for fixed values, which lowered the number of variables, thus decreasing execution time. Fixing variables was a way of simplifying the models, this exemplified the trade-off between model accuracy and execution time.

### 2.1 Program structure

To facilitate future implementations, the program is structured around model functions, which can be utilized in any order. The models are divided into five categories: layout models, component sizing models, efficiency models, auxiliary models, and a scoring model. Table 2.1 presents the different models that the transmission optimization tool consists of.



**Table 2.1:** The optimization tool's different models.

<b>Models</b>	
<i>Layout models</i>	
	Two-stage layshaft
	Three-stage layshaft
	Multi-speed two-stage layshaft
	Multi-speed three-stage layshaft
<i>Component sizing models</i>	
	Gear-set sizing model
	Shaft sizing model
	Bearing sizing model
<i>Efficiency models</i>	
	Gear power loss model
	Bearing power loss model
	Seal power loss model
	System efficiency model
<i>Auxiliary models</i>	
	Differential assembly model
	Motor assembly model
	Shifting element model
	Packaging models
<i>Scoring model</i>	
	Scoring model

The **layout models** represent the transmission layouts modeled in this thesis. Inside the layout models the different components, e.g. gears and shafts, are defined. The layout models will present an optimal layout solution.

**Component sizing models** use input data, such as torque and angular velocity, to calculate optimal sizing for each component.

**Efficiency models** calculate the power loss associated with each component, as well as the total system efficiency for the entire mechanical transmission.

**Auxiliary models** are simple models for the electric motor, differential, and shifting elements. These were developed to capture dimensions and potential constraints caused by these components. Packaging models include calculations for the outer dimensions of the transmission system.

Lastly, a **scoring model** is used to determine the optimal solution of a certain population, based on the optimization objectives.

## 2.2 Layout models

The layout of the mechanical transmission defines the general structure of the system, as well as the included components. Layout models utilizes component models, which correspond to the components of the specific layout model. Thereby, the layout model defines the order in which calculations of components are made, and acts as an interface between the different components.

### 2.2.1 Layshaft models

Layshaft transmissions consist of one or more offset gear-sets. If several gear-sets are used in series, referred to as multi-stage, the total gear ratio is the product of the gear-sets respective gear ratios. A multi-stage layshaft transmission can reach a relatively high gear ratio, without

particularly high gear ratios for each stage, which decreases the gears' size. However, by having more stages there are more gears, thus an increased amount of shafts and bearings needed, which results in increased mass [15].

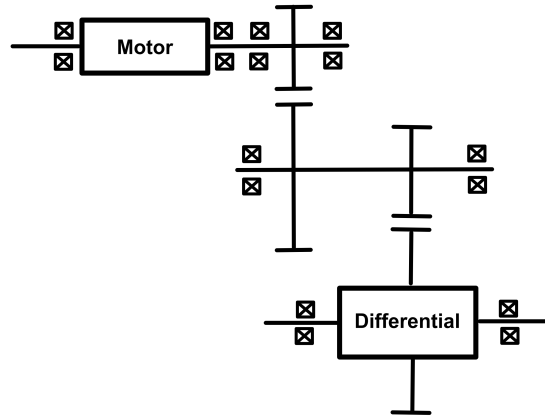


**Figure 2.2:** Two-stage layshaft layout.

The two-stage layshaft transmission in Figure 2.2, has a number of components that need to be modeled. Figure 2.3 describes the structure of the two-stage layshaft model.

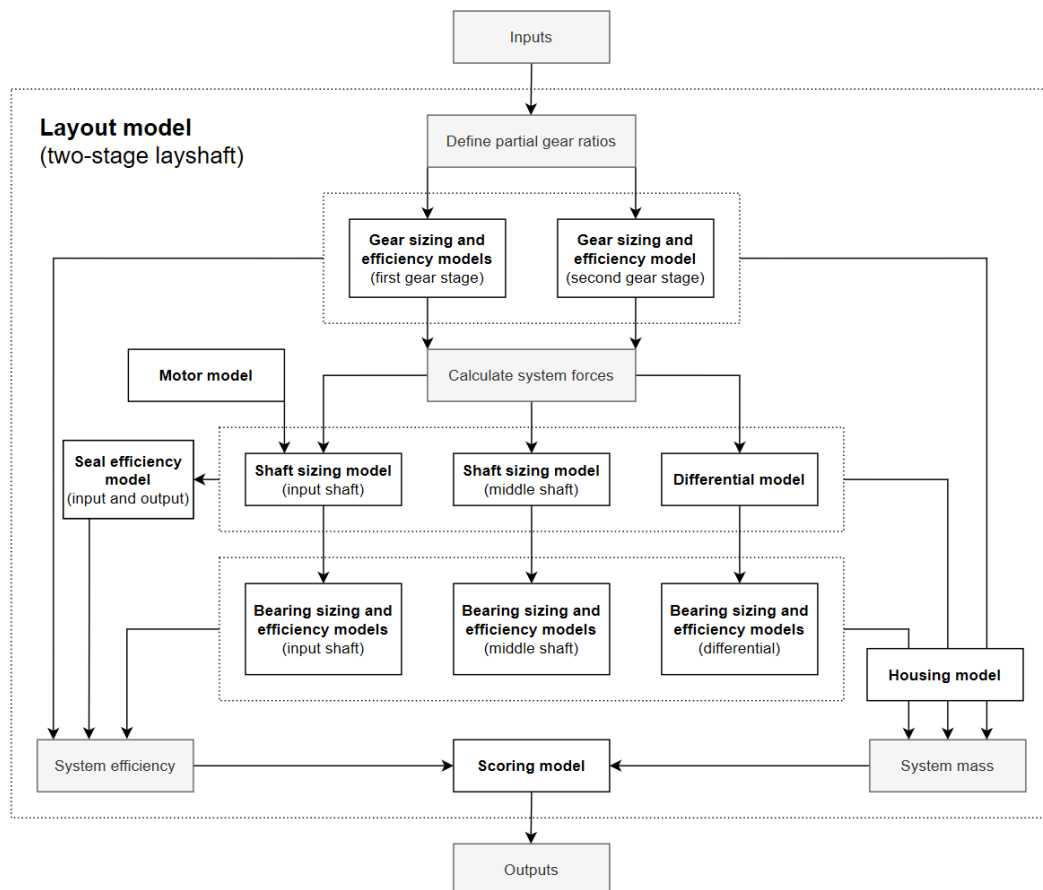


**Figure 2.3:** Structure of the two-stage layshaft layout model in the transmission optimization tool.

As Figure 2.3 shows, the layout model consists of calls to components in a certain order which

ensures dependencies between components are considered. For example, the gears' geometry need to be determined before the system forces can be calculated. By varying the gears' geometry, different system solutions can be produced. Results of all components' mass and efficiency are used in the scoring model to determine the score of a certain system solution.

Partial gear ratios are the gear ratios for the different gear-sets in a multi-stage layshaft transmission, which together multiplies to become the total gear ratio. The method for deciding on partial gear ratios is explained in Section 2.2.3 "Partial gear ratios of layshaft transmissions".

There is potential to increase the number of different speeds of a layshaft transmission. This was modeled according to Section 2.2.2 "Multi-speed layshaft models".

### 2.2.2 Multi-speed layshaft models

In Figure 2.4 the design of a multi-speed two-stage layshaft transmission is presented. The design of a multi-speed layout can vary, but the design in Figure 2.4 was used for all multi-speed layout models in this thesis.

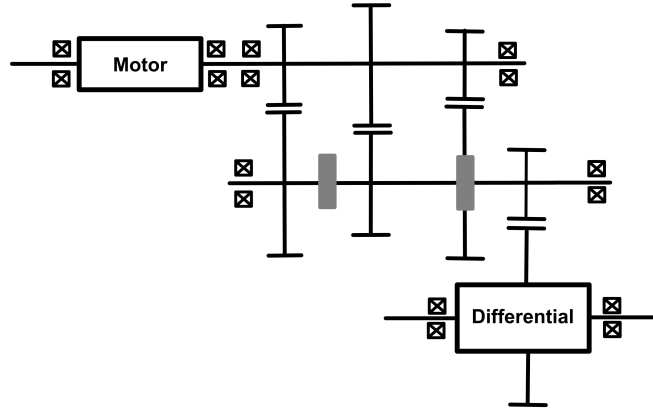


**Figure 2.4:** Multi-speed two-stage layshaft layout.

The layout model of the multi-speed layshaft transmission is similar to the single-speed layshaft model described in Figure 2.3. However, in order to have several different sets of gears on two parallel shafts, it is necessary for the gear-sets to have the same center distances, which limits the design of the gears. The common center distance is based on the gear-set with the highest gear ratio, as it contains the greatest mesh forces and consequently largest gears. The other gear-sets of lower gear ratios will be able to match the center distance, although some of the gears may be bigger than necessary.

### 2.2.3 Partial gear ratios of layshaft transmissions

For layouts with multi-stage transmissions, e.g. as in Figure 2.2, the partial gear ratios determine the mass of each stage. According to Vu [16], there is an optimal gear ratio partition for a transmission, when minimizing its total mass.

Equation 1 was used to approximate the mass,  $M_{tot_N}$ , of a multi-stage transmission with  $N$  stages. The equation is adapted from Vu [16] and re-written in cumulative format.

$$M_{tot_N} = \pi \rho \sum_{n=1}^N \frac{2(u_n + 1)T_{p,n} (e_1 + e_2 u_n^2)}{u_n K_{0n}} \quad (1)$$

where  $T_{p,n}$  is the allowable torque on the shaft,  $K_{0n}$  is the allowable load intensity factor,  $\rho$  is the density of the gears,  $d_{w_{1n}}$  is the pitch diameter of the pinion,  $u_n$  is the gear ratio, and  $e_1$  and  $e_2$  is the volume coefficients of pinion and wheel, respectively.

In the case of a two- and three-stage transmission, the masses were calculated as:

$$\begin{cases} M_{tot_2} = M_1 + M_2 \\ M_{tot_3} = M_1 + M_2 + M_3 \end{cases} \quad (2)$$

where  $M_1$ ,  $M_2$ , and  $M_3$  are the three different masses for each gear stage and  $M_{tot_2}$  and  $M_{tot_3}$  are the total masses for a two- and three-stage gear train, respectively.

Substitutions were made for unknown parameters in Equation 1. Volume coefficients  $e_1 = e_2 = 1$ , since the gears were approximated as solid cylinders.  $K_0$  was assumed equal for every gear stage, and the torques for all gear stages were expressed in  $T_{1,1}$  (the input torque to the first gear-set) and the partial gear ratios,  $u_n$ , of the other stages.

The total mass in Equation 2, could after substitutions be expressed as Equation 3.

$$\begin{cases} M_{tot_2} \propto \frac{1+u_1}{u_1}(1+u_1^2) + u_1 \frac{1+u_2}{u_2}(1+u_2^2) \\ M_{tot_3} \propto \frac{1+u_1}{u_1}(1+u_1^2) + u_1 \frac{1+u_2}{u_2}(1+u_2^2) + u_1 u_2 \frac{1+u_3}{u_3}(1+u_3^2) \end{cases} \quad (3)$$

where  $u_1$ ,  $u_2$ , and  $u_3$  are the partial gear ratios for each respective gear stage.

Partial gear ratio  $u_2$  in  $M_{tot_2}$  of Equation 3 is substituted with  $\frac{U}{u_1}$  and  $u_3$  in  $M_{tot_3}$  of Equation 3 is substituted with  $\frac{U}{u_1 u_2}$ , which results in Equation 4.

$$\begin{cases} M_{tot_2} \propto u_1 + \frac{u_1^2}{U} + \frac{U^2}{u_1} + U + 1 + \frac{1}{u_1} + u_1^2 + u_1 \\ M_{tot_3} \propto \frac{1+u_1}{u_1}(1+u_1^2) + u_1 \frac{1+u_2}{u_2}(1+u_2^2) + u_1 u_2 \frac{1+(\frac{U}{u_1 u_2})}{\frac{U}{u_1 u_2}}(1+(\frac{U}{u_1 u_2})^2) \end{cases} \quad (4)$$

where  $U$  is the desired gear ratio for the whole transmission gear. The partial gear ratios  $u_n$  in Equation 4 are determined by minimizing the total mass of the whole transmission,  $M_{tot}$ .

#### 2.2.4 Gear mesh frequency

The gear mesh frequency, GMF, was calculated according to Equation 5 from Lecinski [17] and was used as an output parameter from the transmission optimization tool.

$$GMF_n = \frac{z_{p_n} \cdot n_n}{60} \quad (5)$$

where  $GMF_n$  is the gear mesh frequency,  $z_{p_n}$  is number of teeth on the pinion, and  $n_n$  is the pinion rotational speed, of the  $n^{th}$  gear stage.

### 2.3 Gear sizing model

The models for gear sizing are based on the ISO 6336 standard [18]. The method for gear sizing used in this thesis was "Method B" of ISO 6336.

The gears' mass were calculated by approximating the gears as homogeneous cylinders according to Equation 6.

$$m = \rho \pi b \frac{d^2}{4} \quad (6)$$

where  $m$  is the mass,  $\rho$  is the density,  $b$  is the width, and  $d$  is the reference radius of the gear.

### 2.3.1 Contact stress limitation

According to ISO [19], the contact stress,  $\sigma_H$ , was calculated separately for pinion and wheel, and was done according to Equation 7, 8, and 9.

$$\sigma_{H0} = Z_H Z_E Z_\varepsilon Z_\beta \sqrt{\frac{F_t U + 1}{d_p b U}} \quad (7)$$

$$\sigma_{H \text{ pinion}} = Z_B \sigma_{H0} \sqrt{K_A K_\gamma K_v K_{H\beta} K_{H\alpha}} \quad (8)$$

$$\sigma_{H \text{ wheel}} = Z_D \sigma_{H0} \sqrt{K_A K_\gamma K_v K_{H\beta} K_{H\alpha}} \quad (9)$$

where  $F_t$  is the transverse tangential load,  $b$  is the face width,  $d_p$  is the pinion diameter, and  $U$  is the gear ratio.  $K_A$ ,  $K_\gamma$ ,  $K_v$ ,  $K_{H\beta}$ ,  $K_{H\alpha}$  are general influence factors described in ISO [18], and originates from the gears' operating conditions.

Equation 10 is used for calculating the pitting stress limit,  $\sigma_{HG}$ , from the allowable contact stress,  $\sigma_{H \text{ lim}}$ .

$$\sigma_{HG} = \sigma_{H \text{ lim}} Z_{NT} Z_L Z_V Z_R Z_W Z_X \quad (10)$$

The contact stress factors,  $Z$ , were used to scale the contact stress depending on gear geometry and operating conditions, according to ISO [19]. Assumed values of the general influence factors and contact stress factors can be seen in Table A.1 in Appendix.

### 2.3.2 Bending stress limitation

The gears' tooth bending strength, was restricted by the stress in the tooth root. In accordance with ISO [20], the tooth root stress was calculated with the addition of several influence factors.

Where the tooth root stress,  $\sigma_F$ , was calculated with Equation 12.

$$\sigma_{F0} = \frac{F_t}{b m_n} Y_F Y_S Y_\beta Y_B Y_{DT} \quad (11)$$

$$\sigma_F = \sigma_{F0} K_A K_\gamma K_v K_{F\beta} K_{F\alpha} \quad (12)$$

where  $F_t$  is the transverse tangential load,  $b$  is the gears' face width, and  $m_n$  is the normal module.

The tooth root stress limit,  $\sigma_{FG}$ , was calculated from the allowable tooth root stress,  $\sigma_{F \text{ lim}}$ , according to Equation 13.

$$\sigma_{FG} = \sigma_{F \text{ lim}} Y_{ST} Y_{NT} Y_{\delta \text{ rel} T} Y_{R \text{ rel} T} Y_X \quad (13)$$

General influence factors for tooth bending,  $K_{F\beta}$  and  $K_{F\alpha}$ , can be seen in Table A.1 in Appendix, together with the bending stress factors,  $Y$ , which were calculated according to ISO [20].

### 2.3.3 Constraints for gears

#### Hunting tooth ratio

In order to achieve a hunting tooth ratio, the tooth numbers are chosen to be relatively prime, as discussed by Dudley [21].

#### Durability constraints

There are two primary constraints for the durability of the gears. Firstly, the ratio between the pitting stress limit,  $\sigma_{HG}$ , and the contact stress,  $\sigma_H$ , must be greater than the safety factor for contact pressure,  $S_H$ .

$$\frac{\sigma_{HG}}{\sigma_H} > S_H \quad (14)$$

Secondly, the ratio between the tooth root stress limit,  $\sigma_{FG}$ , and the tooth root stress,  $\sigma_F$ , must be greater than the safety factor for bending,  $S_F$ .

$$\frac{\sigma_{FG}}{\sigma_F} > S_F \quad (15)$$

#### Further constraints

Further constraints are defined to ensure that the gears operate without undercut, interference, and that the tooth thickness is greater than zero at the tip radius.

The rim thickness,  $s_R$ , of a gear is a measurement for how much material exists beneath the tooth root, where the material's width is equal to the face width of the teeth [20]. Figure 2.5 depicts the gear rim.

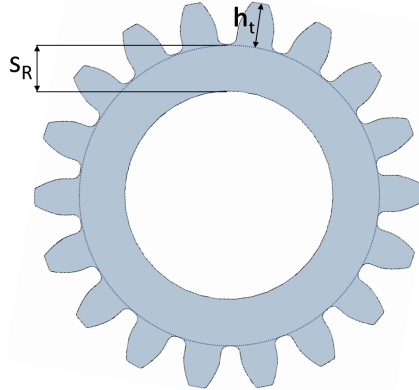


**Figure 2.5:** Rim thickness and tooth height of a gear.

To not influence the bending stress in the teeth the minimum rim thickness was selected to fulfill Equation 16, in accordance with ISO [20].

$$s_R \geq 1.2h_t \quad (16)$$

where  $h_t$  is the tooth height.

Lastly, there are some design constraints which were defined by BorgWarner, for example minimum transverse and total contact ratio. BorgWarner's gear design constraints are based on testing and experience from designing power transmission units, and ensure desirable operating and manufacturing conditions. Values for these constraints are left out of this report as they are confidential property of BorgWarner.

## 2.4 Models for sizing of other components

Other components in the transmission system are shafts, bearings, and seals. The shafts and bearings were sized to withstand mesh loads and torques without failing due to mechanical overload. Seals were neglected from sizing in this thesis.

### 2.4.1 Shaft sizing model

The method used for the sizing of the shafts includes the von Mises simplified mean stress equation, which can be found in ANSI/AGMA [22].

The maximum bending moment and the input torque determines the minimum diameter of the shaft, with regards to the maximum allowable stress divided with a safety factor. The minimum diameter of the shaft was calculated according to Equation 17

$$d_{sh,min} = \left( \frac{\sqrt{(K_{ts}32M)^2 + 3(K_{tnom}16T)^2}}{\pi\sigma_{allow}} \right)^{1/3} \quad (17)$$

where  $d_{sh,min}$  is the minimum allowable diameter of the shaft,  $K_{ts}$  and  $K_{tnom}$  are the stress concentration factors for the bending moment and the torque, respectively,  $M_b$  is the bending moment,  $T$  is the torque on the shaft, and  $\sigma_{allow}$  is the limited stress divided by a safety factor,  $\frac{\sigma_{lim}}{F_S}$ .

The length of the shaft was determined by the number of components on the shaft, with a specified clearance between every component. Both diameter and length of the shaft depends on the selected bearings.

### 2.4.2 Bearing sizing model

The bearings used in the model were selected from a database of deep groove ball bearings from the SKF product catalog [23]. Therefore, sizing was done according to SKF [23].

The approach used the minimum shaft diameter, as a minimum inner diameter for the bearing. The bearing with the lowest mass, that could sustain the loads, was chosen. If the bearing's inner diameter was greater than the shaft diameter, the additional mass of an increase in shaft diameter was also taken into consideration when selecting bearings.

### 2.4.3 Auxiliary component models

#### Differential assembly model

A simple model to simulate the differential was added for rough geometry and mass of the component. The geometry was necessary to capture interactions between the differential and other components, such as the bearings supporting the differential, and gears that may interfere with the differential.

The differential was seen as part of the transmission system, thus the differential's mass was included in the transmission system's mass. The power losses of the differential were not included in the system's power loss for the transmission system.

The differential type can be decided depending on if the output shafts should be parallel or perpendicular to the motor.

#### Motor assembly model

Similarly to the differential assembly model, the motor model defines geometry of the motor to capture possible interference with other components. The motor's mass, efficiency, and dimensions were not included in the transmission system.

### Shift element model

The shift elements are components on the multi-speed transmissions' input shaft, and determine which gear is transferring power. In order to capture the characteristics of the shift elements they were added as a model. However, no real investigation was made to determine exact geometry or mass of the shift elements, thus their mass is excluded from the total system mass.

#### 2.4.4 Packaging models

##### Diversion angle

The diversion angle,  $\gamma$ , in Figure 2.6, was calculated with the law of cosines, using the two center distances producing the angle, and the angle's opposing side. The minimum length of the opposing side was based on constraints against collision between components on the first and last shaft.

Similar calculations were done for  $\gamma_1$  and  $\gamma_2$ , in Figure 2.7. However,  $\gamma_1$  was set to a fixed value and  $\gamma_2$  was minimized without causing collision of components. Ideally both angles should be optimized, but since no optimization objective for packaging was developed it was not possible to find an optimal combination of the two angles.

##### Outer dimensions of transmission system

The outer dimensions of the transmission system are output parameters of the transmission optimization tool.

The method used the largest gear on each shaft to define outer boundaries of the transmission system. In Figure 2.6 the two dimensions  $L$  and  $H$ , length and height, are illustrated. The dimensions were calculated with Equation 18.

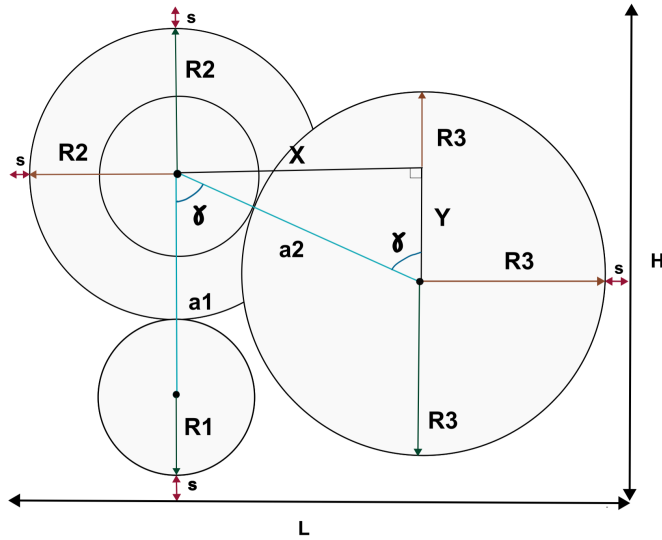


Figure 2.6: Outer dimensions of a two stage layshaft model.

$$\begin{cases} L_{2Stage} = R_1 + a_1 + R_2 + 2s + 2t \\ H_{2Stage} = R_2 + X + R_3 + 2s + 2t \end{cases} \quad (18)$$

where  $L_{2Stage}$  is the length,  $H_{2Stage}$  is the height,  $a_1$  is the center distance of the first gear stage,



$a_2$  is the center distance of the last gear stage,  $\gamma$  is the diversion angle,  $s$  is the component gap, and  $t$  is the housing's wall thickness.

Approximation of the outer dimensions of a three stage layshaft layout was done in a similar way, as can be seen in Figure 2.7.

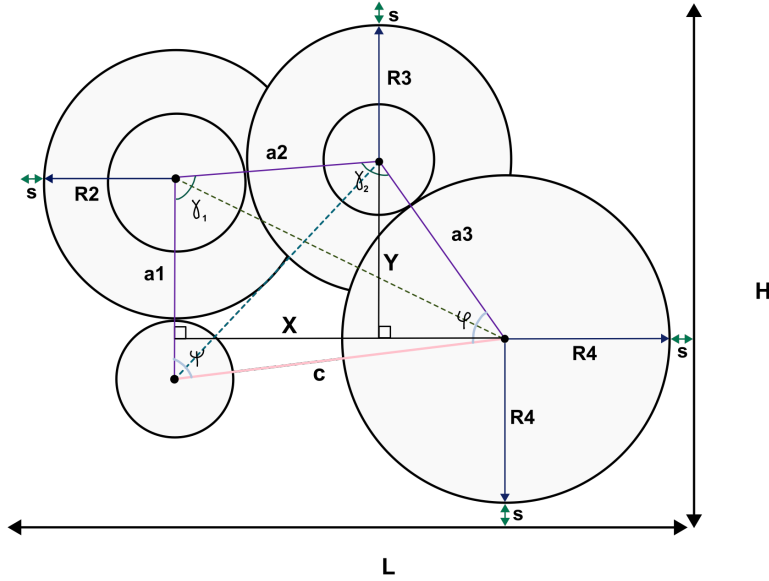


**Figure 2.7:** Outer dimensions of a three stage layshaft model.

The length,  $L_{3Stage}$ , and height,  $H_{3Stage}$  was calculated as Equation 19.

$$\begin{cases} L_{3Stage} = R_2 + X + R_4 + 2s + 2t \\ H_{3Stage} = R_3 + Y + R_4 + 2s + 2t \end{cases} \quad (19)$$

The third dimension was the width,  $W$ , which was approximated as the length of the longest shaft,  $l$ , in the layshaft model. Equation 20 was used in all layshaft models.

$$W = l + 2s + 2t \quad (20)$$

### Approximation of housing mass

The outer dimensions of the transmission systems were utilized to get a rough estimate on the amount of material needed for a housing. Length, height, and width were used to get the volume of the gearbox according to Equation 21 and then calculate the approximated mass of the housing made of aluminum according to Equation 22.

$$V = L \cdot W \cdot H - (L - 2t)(W - 2t)(H - 2t) \quad (21)$$

$$m_{housing} = \rho \cdot V \quad (22)$$

## 2.5 Component efficiency models

Power losses are commonly split up into load and non-load dependent losses [24, 25, 26, 27]. Which was done according to Table 2.2.

**Table 2.2:** The power loss equations used for component models.

Power loss	Symbol	From reference
Gears loaded losses	$P_M$	ISO [26] and ISO [28]
Gear non-loaded losses	$P_{GW}$	ISO [26]
Bearings loaded losses	$P_B$	ISO [26]
Bearings non-loaded losses	$P_{BW}$	ISO [26]
Oil seal losses	$P_{VD}$	Fernandes [27]

Power losses which ISO [26] also includes are pump and shaft losses were neglected in this thesis.

### 2.5.1 Load dependent losses

#### Gear loaded losses

Gear loaded losses assumed in this thesis originates from friction in the gear mesh. The equation for gear mesh power loss from ISO [26]:

$$P_M = \frac{f_m T_p n_p \cos^2 \beta_w}{9549M} \quad (23)$$

where  $P_M$  is the mesh power loss,  $f_m$  is the mesh friction coefficient,  $T_p$  is the torque on the pinion,  $n_p$  is the rotational speed of the pinion,  $\beta_w$  is the operating helix angle, and  $M$  is the mesh mechanical advantage.

The coefficient of friction in ISO [28] defined by Schlenck (Equation 24), which approximates an average constant coefficient of friction over the path of contact, was used.

$$f_m = \mu_{mz} = 0.048 \left( \frac{F_{bt}/b}{v_{\Sigma C} \rho_{redC}} \right)^{0.2} \eta_{oil}^{-0.05} R_a^{0.25} X_L \quad (24)$$

where  $F_{bt}$  is the tangential force at the base circle,  $b$  is the tooth width,  $v_{\Sigma C}$  is the sum speed at the operating pitch circle,  $\rho_{redC}$  is the reduced radius of the curvature at the pitch point,  $\eta_{oil}$  is the dynamic oil viscosity,  $R_a$  is the arithmetic mean roughness, and  $X_L$  is a factor for the oil type.

### Bearing loaded losses

Bearing friction torque,  $M_B$ , estimation from ISO [26] (Equation 25) was used to determine the loaded power loss of the bearings.

$$M_B = \frac{f_B(P)^i(d_m)^j}{1000}, \quad (25)$$

where the coefficient of friction,  $f_B$ , is selected from ISO [26],  $P$  is the bearing dynamic load,  $d_m$  is the bearing mean diameter, and  $i$  and  $j$  are exponents dependent on bearing type.

The friction torque was multiplied with the rotational speed of the bearing, in Equation 26, to determine the power loss.

$$P_B = \frac{M_B n}{9549} \quad (26)$$

### 2.5.2 Non-load dependent losses

Non-load dependent power losses included in the models were windage and oil churning power losses on gears and bearings, and oil seal power losses.

#### Windage and churning losses

The gear windage and churning losses were adapted from ISO [26], where losses from the face of the gears,  $P_{GW_1}$ , and from the tooth surfaces,  $P_{GW_2}$ , were calculated individually. Equation 27 was used for the face of the gears and Equation 28 was used for the tooth surfaces of the gears.

$$P_{GW_1} = \frac{1.474 f_g \nu n^3 D^{5.7}}{A_g 10^{26}} \quad (27)$$

$$P_{GW_2} = \frac{7.37 f_g \nu n^3 D^{4.7} b \frac{R_f}{\sqrt{\tan \beta}}}{A_g 10^{26}} \quad (28)$$

where  $f_g$  is the gear dip factor,  $\nu$  is the oil viscosity,  $n$  is the rotational speed of the element,  $A_g$  is the arrangement constant,  $R_f$  is the roughness factor,  $b$  is the total face width,  $D$  is the outside diameter of the element, and  $\beta$  is the helix angle.

The power loss equation for the windage and churning of the bearings,  $P_{BW}$ , are also found in ISO [26].

#### Oil seal losses

The oil seal power loss function in Equation 29 described by Schlegel and Hösl [24], defined by H. Linke, was used.

$$P_{VD} = [145 - 1.6\theta + 350 \log(\log(\nu_{40^\circ} + 0.8))] \cdot 10^{-16} \cdot d_{sh}^2 \cdot n \quad (29)$$

where  $P_{VD}$  is the power loss of the oil seal,  $\theta$  is the temperature,  $\nu_{40^\circ}$  is the oil viscosity at 40°C, and  $d_{sh}$  is the shaft diameter.

## 2.6 Scoring model

A scoring model was developed to combine the two objectives, minimization of mass and power losses, to a single comparable metric. It was established that the power consumption caused by increased mass could be compared with the power consumption from power losses inside the transmission system.

The efficiency power loss factor,  $\eta_P$  was calculated by dividing the output power with the input power, as shown in Equation 30.

$$\eta_P = \frac{P_{out}}{P_{in}} = \frac{P_{in} - P_{loss}}{P_{in}} \quad (30)$$

where  $P_{loss}$  is the sum of all component power losses from Table 2.2.

The mass' effect on power consumption was calculated by comparing the required power to keep a vehicle at a certain speed depending on the vehicle's mass. Equation 31 shows the external forces assumed to affect the vehicle.

$$P_{wheels} = (F_{drag} + F_{roll})v \quad (31)$$

$$\text{where } F_{drag} = C_d A \frac{\rho_a v^2}{2}, \text{ and } F_{roll} = \mu mg. \quad (32)$$

Substitution of the parameters in Equation 31 with Equation 32, gave a function of power depending on additional mass, seen in Equation 33.

$$P(m) = C_d A \frac{\rho v^3}{2} + (m_0 + m)g\mu v \quad (33)$$

The factor for power loss caused by increasing the vehicle's mass by one kilogram, was calculated below by utilizing Equation 33, and the parameter values in Table 2.3.

$$\eta_m = \frac{P(0)}{P(1)} = 0.9998 \quad (34)$$

**Table 2.3:** Parameters and parameter values for estimation on the mass' effect on the power consumption, in the example in Equation 34.

Parameter	Symbol	Value for example
Vehicle speed	$v$	30 $m/s$ (highway driving)
Coefficient of drag	$C_d$	0.3 (common for passenger cars [29])
Vehicle front area	$A$	2 $m^2$ (approximation for passenger car)
Air density	$\rho_a$	1.25 $kg/m^3$ (at 10°C)
Rolling resistance	$\mu$	0.01 (driving on smooth asphalt or concrete[30])
Vehicle mass	$m_0$	1 800 $kg$ (approx. mass of Tesla Model 3 [31])
Constant of gravity	$g$	9.81 $m/s^2$
Additional mass	$m$	- $kg$

The result of Equation 34 suggested that, for the parameters used in the example, the power consumption increase of adding one kilogram of mass to the vehicle corresponded to an efficiency

factor of 0.9998. Similarly, in the scoring model the  $\eta_m$  factor is calculated based on the mass of the current component or transmission system being scored.

When comparing different solutions, the mass power loss factor,  $\eta_m$ , and efficiency power loss factor,  $\eta_P$ , were multiplied to get the total score, as in Equation 35.

$$\text{score} = \eta_P \cdot \eta_m \quad (35)$$

## 2.7 Optimization process

The transmission optimization was based on two levels of optimization. Since most transmission layouts contain several gear-sets, a separate gear-set optimization was made in the gear-set model, which output the optimal gear-set solution for the given input data and potential design constraints. The other optimization process was a system optimization, which evaluated the different components' impact on other components and selected those that optimized the system as a whole.

### 2.7.1 Gear-set optimization

Gears were optimized by varying multiple design parameters simultaneously, these are specified in Table 2.4. Values for the constant parameters in Table 2.4 were based on standard values from ISO [32].

**Table 2.4:** Variable and constant design parameters for gear design.

Variable parameters	Symbol	Selected values	Unit
Normal module	$m_n$	0.5, 0.55 ... 3.0	mm
Number of teeth (pinion)	$z_p$	$z_{min}, z_{min} + 1 \dots z_{max}/U^*$	-
Face width coefficient	$b_0$	10, 11 ... 20	-
Helix angle	$\beta$	10, 11 ... 30	°
Pressure angle	$\alpha_n$	15, 16 ... 25	°
Profile shift coefficient (pinion)	$x_{0,p}$	-0.7, -0.6 ... 0.7	-
Profile shift coefficient (wheel)	$x_{0,w}$	-0.7, -0.6 ... 0.7	-
<b>Constant parameters</b>			
Addendum coefficient	$h_{aP}$	1.00	-
Dedendum coefficient	$h_{fP}$	1.25	-
Root radius coefficient	$\rho_{fP}$	0.35	-

\* $z_{max}$  is the maximum number of teeth allowed on any gear. If the gear ratio is  $U > 1$ , the maximum value for  $z_p$  is decided in order that the number of teeth on the wheel  $z_w \leq z_{max}$ .

Ranges for normal module, and face width coefficient were defined as in Table 2.4 after starting with wider ranges and identifying what values the optimized solutions tended to have.

The range for number of teeth were decided based on experience from BorgWarner, and are therefore only shown as symbols. However, to give some perspective  $z_{min} \approx 10$  and  $z_{max} \approx 100$ .

Ranges for helix and pressure angle were selected based on values validated according to ISO [18]. Miler et al. [33], Samya et al. [34], and Rai et al. [35] all selected the range  $-0.7$  to  $0.7$  for profile shift, thus it was used for the gear optimization in this thesis.

The length of the parameter ranges in Table 2.4 are not the same for every parameter. This is further discussed in Section 4.3.1.

Figure 2.8 shows a schematic overview of the gear-set optimization. The following paragraphs describe the steps of the optimization process.

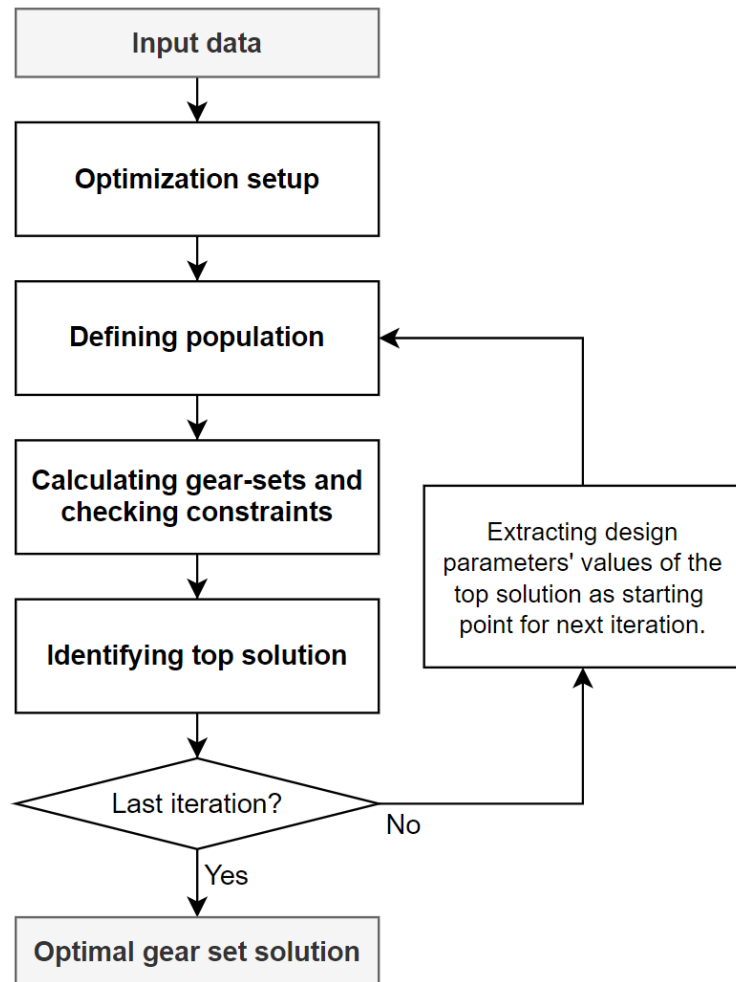


**Figure 2.8:** Process for gear-set optimization.

**Optimization setup.** Defining the ranges for design variables, as in Table 2.4, and the number of iterations for the gear optimization.

**Defining population** consisting of unique combinations of design variables, for the current iteration.

**Calculating gear-sets** from the population and **checking constraints** for the gear-sets, and removing gear-sets failing to clear the constraints.

**Identifying top solution** of the current iteration, by utilizing the scoring model.

### Example of gear-set optimization

In Figure 2.9 the iteration process is illustrated. For the sake of simplicity, the number of design parameters were reduced to two ( $z_p$  and  $m_n$ ). For this example, ranges for design parameters were according to Equation 36, and the number of iterations was three.

$$\begin{cases} z_p = [20, 21, \dots, 34] \\ m_n = [1.0, 1.1, \dots, 2.0] \end{cases} \quad (36)$$

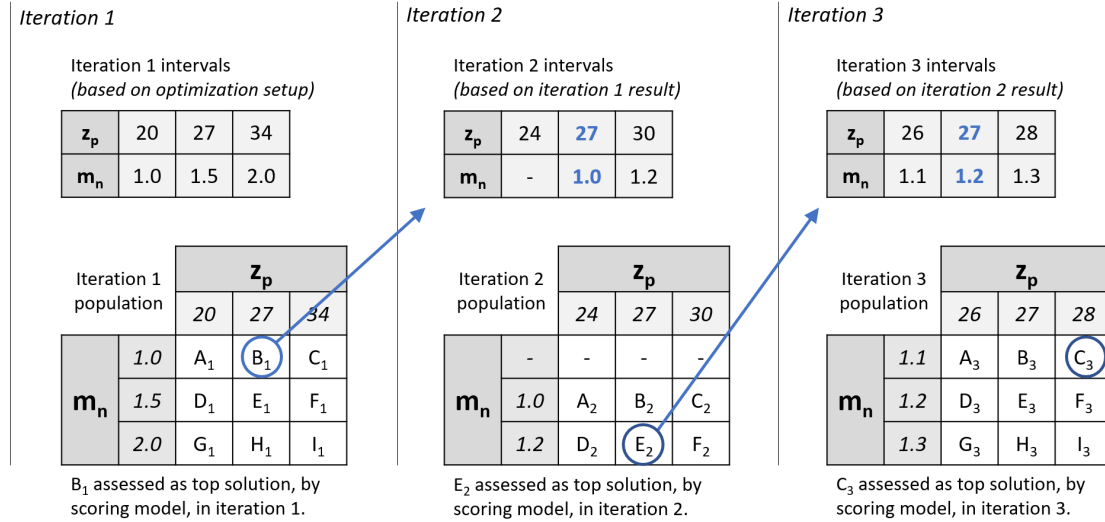


**Figure 2.9:** Iteration process of a simplified gear-set optimization, corresponding to the example.

The left field in Figure 2.9 represents the first iteration of the gear optimization process. The "iteration 1 intervals" are based on the ranges of the design parameters, where the center of the intervals were selected as the mean values of the defined ranges. The intervals' start and end points were selected as the first and last values of the defined ranges. This ensured that all values of the design parameter ranges were taken into consideration in the optimization process. The step length was the difference between two adjacent values in an interval.

The "iteration 1 population" was created by combining the values for the number of teeth and normal module. The fact that the intervals for design parameters were length three implied that the number of combinations, i.e. population size, was nine ( $3 \cdot 3$ ). The population underwent calculations and constraint checks and a top solution was selected. The top solution in "iteration 1" was "B<sub>1</sub>", defined by the values of design parameters  $z_p = 27$  and  $m_n = 1.0$ .

The second iteration began with creation of "iteration 2 intervals", which were created by originating from the design parameter values of the optimal solution in "iteration 1" ( $z_p = 27$ ,  $m_n = 1.0$ ). From these values the start and end values of the intervals were selected by stepping half the step length of the previous iteration. Resulting intervals were more narrow and had higher resolution than the intervals in the previous iteration. Since the value for normal module of "B<sub>1</sub>" was the minimum of the defined range for normal module, there was no lower value in the interval.

After creating intervals, the population for "iteration 2" was defined. The population's top solution was determined, and its values for the design parameters were used for the next iteration. For "iteration 2" the top solution was "E<sub>2</sub>", defined by  $z_p = 27$  and  $m_n = 1.2$ .

"Iteration 3 intervals" were based on the top solution of the second iteration. However, since "iteration 3" was the final iteration the intervals' step lengths were the same as the step lengths

defined by the design parameter ranges, in Equation 36. The equal step length ensured that the desired level of detail was achieved. Since "iteration 3" was the final iteration its top solution,  $C_3$ , was the overall optimal gear-set solution.

$$\begin{cases} N_{calcs} = 9 + 6 + 9 = 24, & \text{with iteration process.} \\ N_{calcs} = 11 \cdot 15 = 165, & \text{without iteration process.} \end{cases} \quad (37)$$

Equation 37 shows the number of calculations,  $N_{calcs}$ , performed in the iteration process and when calculating every combination from the design parameter ranges in Equation 36.

Figure 2.10 contains a matrix which represents every combination of  $z_p$  and  $m_n$ , corresponding to all gear solutions. Highlighted fields depicts the solutions that were calculated in the iteration process in the example, and for which iteration they were calculated in.

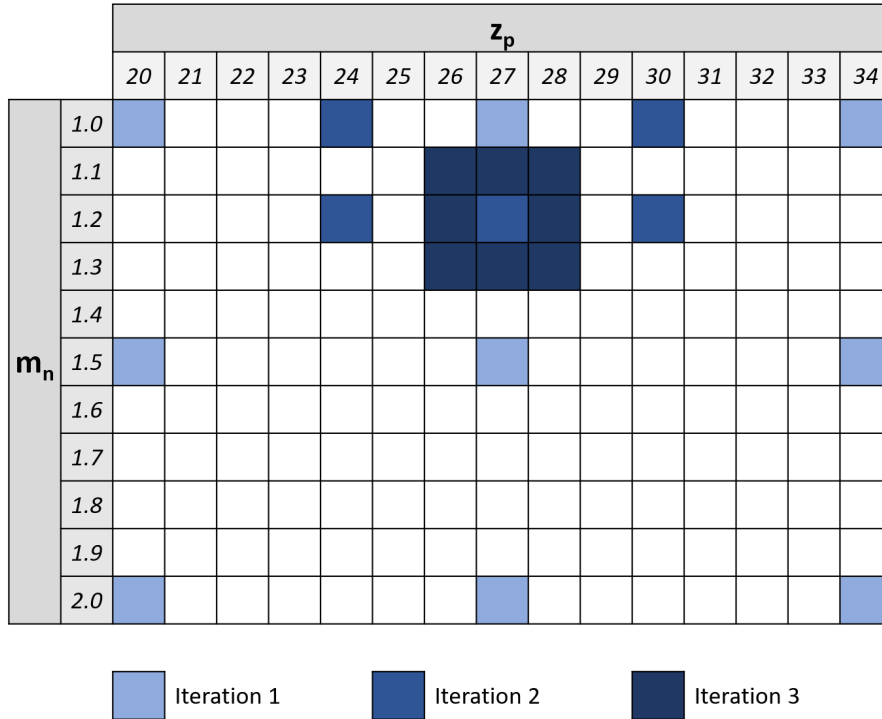


**Figure 2.10:** Visual representation of solutions calculated by using iteration based optimization.

### 2.7.2 System optimization

A population for the system optimization was generated by varying the helix angle separately for every gear-set in the transmission system. Figure 2.11 presents the population of the system optimization for a layout with two gear stages, resulting in a population size equal to the square of the number of helix angles in the defined range.

Gears were optimized, shafts and bearings were calculated and the total mass and power loss of each system solution, of the population, was determined.

The system solutions were ranked with the scoring model, where the highest ranked was appointed as the optimal system solution.



		Helix angle, $\beta$ , of 1st gear stage					
		10	11	12	...	29	30
Helix angle, $\beta$ , of 2nd gear stage	10						
	11						
	12						
	...						
	29						
	30						

Figure 2.11: Population of the system optimization.

## 2.8 Model verification

Sizing and efficiency models were verified by comparing the thesis models' results with models created in MASTA, a commercial software for design, simulation, and analysis of gearbox and driveline systems. MASTA utilized the same method for sizing of gears, which made it possible to verify the dimensions and safety factors of the gears calculated in the transmission optimization tool. MASTA also allowed for a variety of methods for calculating efficiency of mechanical components. These were used to verify the results of the efficiency models in this thesis. Verification was made to ensure that the models had been correctly implemented, and it should not be seen as a validation.

Verification was done by running the optimization tool and subsequently using the output data, such as gears' geometry, to recreate the optimized transmission in MASTA. If values for safety factors, mesh properties, and power loss were similar for the optimization tool and MASTA, the models were deemed as verified.

Data comparison between one example of the optimization tool and MASTA can be found in Table A.2, which was based on input data in 3.1. Some deviations were allowed in safety factor and power loss, since MASTA also consider manufacturing parameters found in ISO [19, 20].

## 2.9 Model evaluation

Execution time and optimization results were evaluated for the cases in Table 2.5. Execution time was measured for all cases, and the impact of fixing variables was evaluated by comparing optimization results from the different cases.

Table 2.5: Cases used for testing the transmission optimization tool for a single-speed two-stage layshaft transmission.

Case no.	Variables	Fixed parameters
Case 0	$z_p, m_n, b_0, \alpha_n, x_{0,p}, x_{0,w}, \beta$	—
Case 1	$z_p, m_n, b_0, \alpha_n, x_{0,p}, x_{0,w}$	$\beta$
Case 2	$z_p, m_n, b_0, \alpha_n$	$\beta, x_{0,p}, x_{0,w}$
Case 3	$z_p, m_n, b_0, x_{0,p}, x_{0,w}$	$\beta, \alpha_n$
Case 4	$z_p, m_n, b_0$	$\beta, \alpha_n, x_{0,p}, x_{0,w}$

### 2.9.1 Testing execution time

Since there was a target for the execution time of the transmission optimization tool, a method of testing the execution time was defined. Execution time of code could vary from run to run, thus an average was calculated from one hundred runs.

Testing of execution time was performed on the finished transmission optimization tool for different amounts of design variables for the gears, as seen in Table 2.5.

### 2.9.2 Evaluating the impact of fixed design variables

The evaluating procedure was based on calculating the difference in power loss and mass of transmission systems, when assigning fixed values for certain design parameters, instead of varying them.

Evaluations were based on the comparing the cases in Table 2.5. The first evaluation was a comparison between running "Case 0" and "Case 1". Then "Case 1" was compared to "Case 2" and "Case 3", separately. Finally, "Case 0" was compared to "Case 4".

The evaluations were carried out on a population of single-speed two-stage layshaft transmissions. The samples making up the population were derived from simulating electric motors with different input torques and desired gear ratios. The input angular velocity was calculated from an assumed power of 250 kW for all motors. The input torque was varied from 100 to 600 Nm, with 50 Nm increments. And the desired gear ratios was varied between 5 and 15, and every integer between. A total of  $11 \cdot 11 = 121$  unique samples were made of every combination of torque and gear ratio.

## 3 Results

### 3.1 Execution time

The results of testing execution time are based on the five cases in Table 2.5.

As can be seen in Figure 3.1, the time to optimize the transmission layouts depend on the number of speeds, where the single-speed transmission is the fastest to execute. However, the execution time was far above the target of  $\sim 100$  ms.

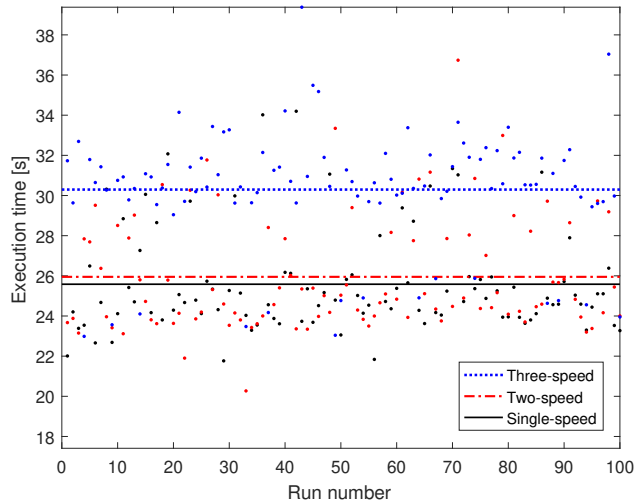


**Figure 3.1:** Execution time of "Case 0". The horizontal lines are mean values of the execution time, for the respective speeds.

When running "Case 1"'s execution time, yet again the execution time was above the targeted time, as can be seen in Figure 3.2.

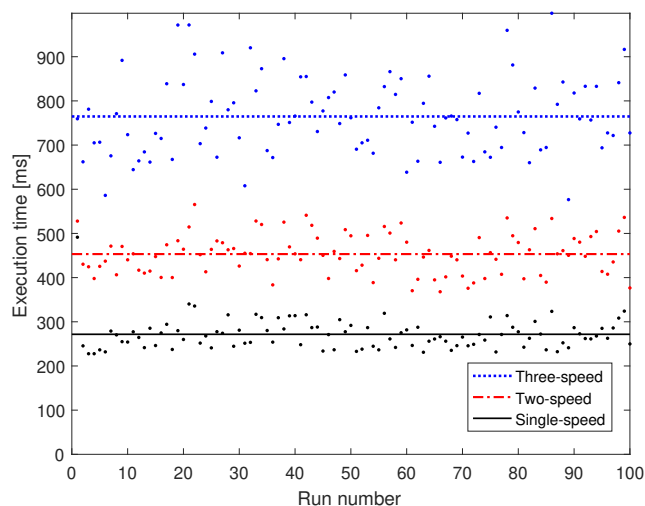


**Figure 3.2:** Execution time of "Case 1". The horizontal lines are mean values of the execution time, for the respective speeds.

Figure 3.3 and 3.4 show that "Case 2" and "Case 3" had the same trend of longer execution time for transmission layouts with more speeds. However, the average execution time was lower for all layouts, compared to "Case 1" (Figure 3.2). Fixing values for pressure angle or profile shift coefficients was not sufficient to lower the execution time below the target.

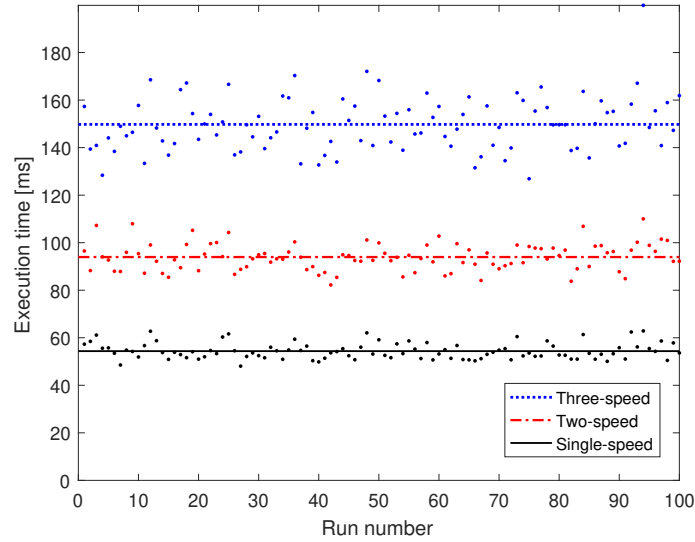


**Figure 3.3:** Execution time of "Case 2". The horizontal lines are mean values of the execution time, for the respective speeds.

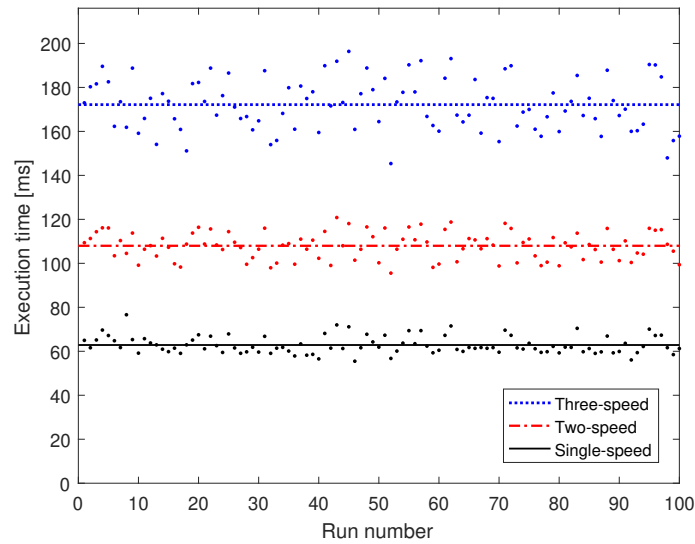


**Figure 3.4:** Execution time of "Case 3". The horizontal lines are mean values of the execution time, for the respective speeds.

Lastly, Figure 3.5 presents the execution times for "Case 4", where the helix angle, pressure angle, and profile shift coefficients were assigned fixed values. Average execution time for optimizing transmission layouts of single- and multi-speeds were all below the targeted execution time.

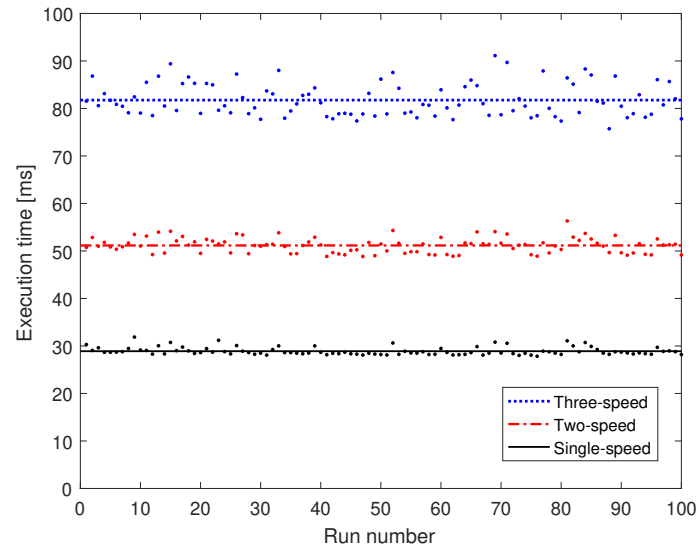


**Figure 3.5:** Execution time of "Case 4". The horizontal lines are mean values of the execution time, for the respective speeds.

## 3.2 Fixed values of design variables

### 3.2.1 Fixed value for helix angle

The fixed values of the helix angles were based on the average helix angles from the optimal system solutions  $\beta = 25^\circ$ .

Figure 3.6 shows the difference in system power loss and mass between "Case 0" and "Case 1", mentioned in Section 2.9 "Model evaluation".

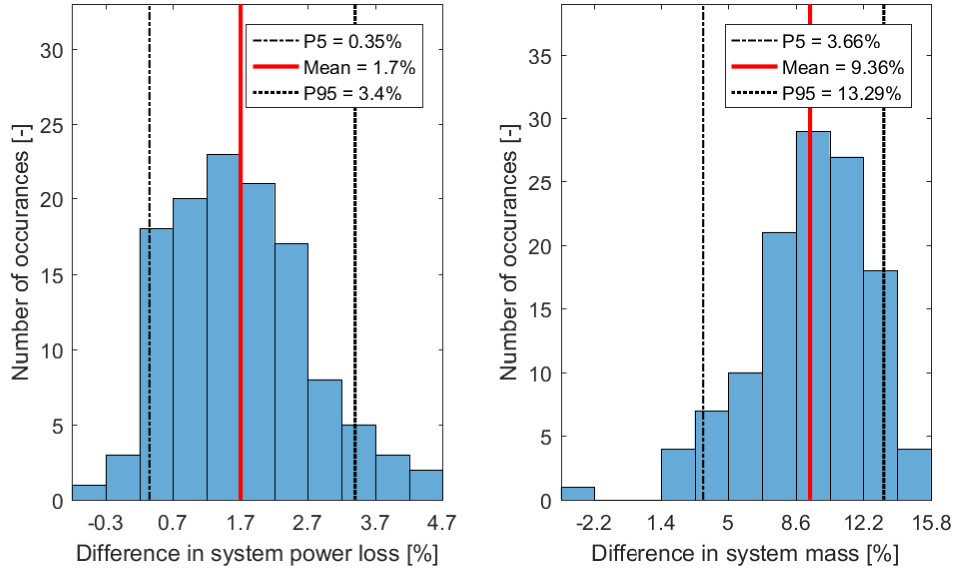


**Figure 3.6:** Increase in system power loss (left) and mass (right) when using a fixed value for helix angle instead of letting the optimizer find optimal values for helix angle.

Figure 3.6 shows that the system power loss in average increases 1.70% with fixed values for helix angles. This translates to an increase in predicted power loss, which was expected since the results are less optimized when fixating design variables' values. The boundaries for the 5th and 95th percentile (P5 and P95) contained 90% of the samples, which indicates that 9 out of 10 transmission systems deviates in power loss between 0.35% and 3.40% compared to the result when varying the helix angle.

Figure 3.6 shows that the system mass in average increases 9.36% when using a fixed values for helix angles. The boundaries for the 5th and 95th percentile indicate that 9 out of 10 transmission systems will deviate in mass between 3.66% and 13.29%.

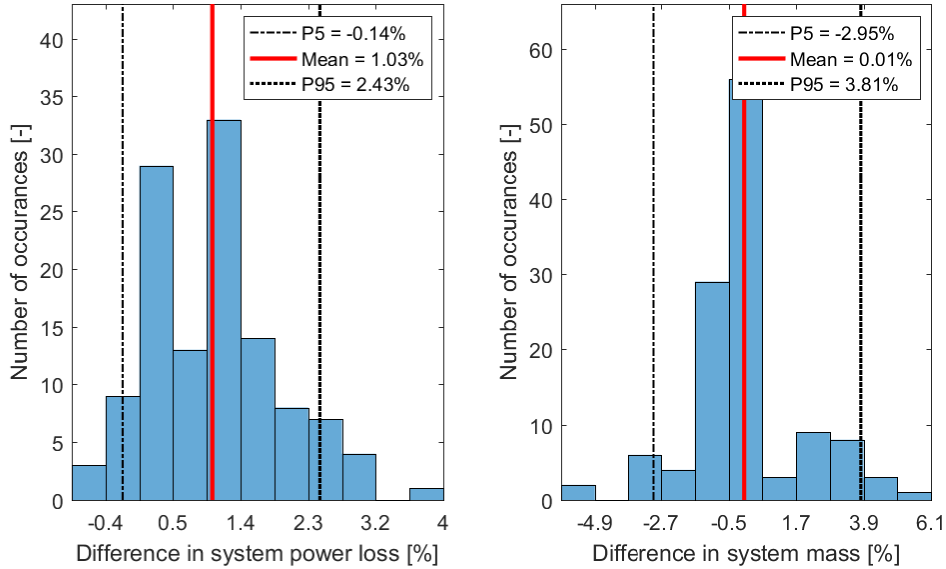
The mean deviation as well as the interval between the 5th and 95th percentile is greater for the difference in system mass, compared to the system power loss. This discrepancy is discussed in Section 4 "Discussion".

The populations used in Figure 3.6 were derived from different input torques and gear ratios. However, the histograms do not show any potential trends between the power loss or mass depending on torque or gear ratio. In order to establish possible dependencies, the data was plotted (Figure A.1 and A.2) and visually checked for any trends, which would suggest dependencies. A trend could for example have been a significantly higher power loss difference for transmission with higher gear ratios, compared to transmission with lower gear ratios. However, no significant trends were discovered.

### 3.2.2 Fixed values for profile shift coefficients

The profile shift coefficients ( $x_{0,p}$  and  $x_{0,w}$ ) were evaluated in a similar way as the helix angle. The same population, as in Section 3.2.1, was analyzed when comparing "Case 1" and "Case 2".

The values for profile shift coefficients for the gears of the optimized system varied widely for different input torques and gear ratios. Instead of selecting the mean values of profile shift coefficients for the fixed value comparison, the value was selected to  $x_p = x_w = 0$ .



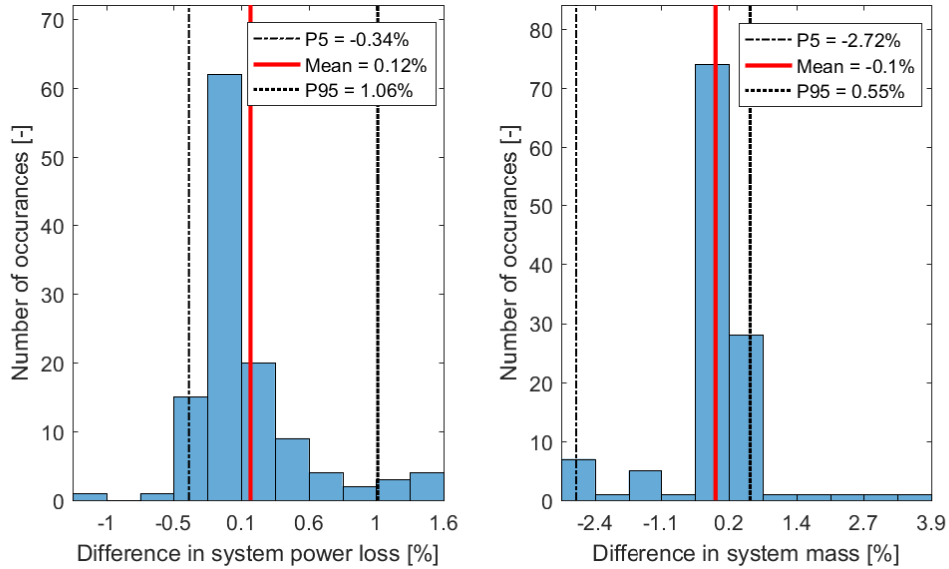
**Figure 3.7:** Increase in system power loss (left) and mass (right) when using fixed value for profile shift coefficients instead of letting the gear optimizer find optimal values.

Figure 3.7 shows that the system power loss in average deviates 1.03% when using fixed values for the profile shift coefficients. Approximately 9 out of 10 transmission systems will deviate in power loss between  $-0.14\%$  and  $2.43\%$  compared to the result when varying the profile shift coefficients.

Figure 3.7 shows that the system mass in average deviates 0.01% when using fixed values for the profile shift coefficients. Approximately 9 out of 10 transmission systems will deviate in power loss between  $-2.95\%$  and  $3.81\%$  compared to the result when varying the profile shift coefficients.

### 3.2.3 Fixed value for pressure angle

The same analysis, as in Section 3.2.2, was made for the pressure angle with the comparison between "Case 1" and "Case 3". The pressure angle was set to  $\alpha_n = 20^\circ$ , since the optimizer commonly used this value for the optimal solution.



**Figure 3.8:** Increase in system power loss (left) and mass (right) when using fixed value for the pressure angle instead of letting the gear optimizer find optimal values.

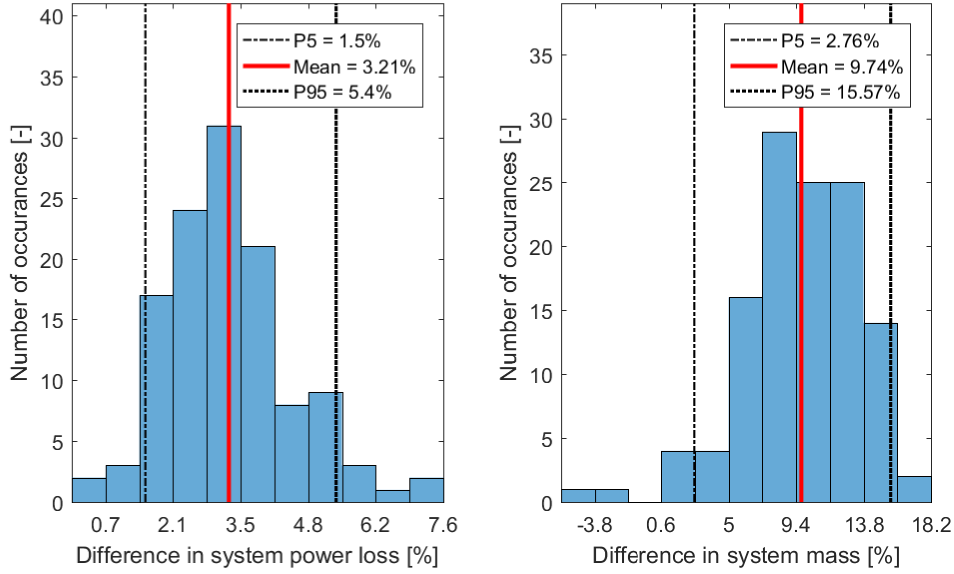
Figure 3.8 shows that the system power loss in average deviates 0.12% when using a fixed value for the pressure angle. Approximately 9 out of 10 transmission systems will deviate in power loss between  $-0.34\%$  and  $1.06\%$  compared to the result when varying the pressure angle.

Figure 3.8 shows that the system mass in average deviates  $-0.1\%$  when using fixed values for the pressure angle. Approximately 9 out of 10 transmission systems will deviate in power loss between  $-2.72\%$  and  $0.55\%$ .



### 3.2.4 Fixed value for helix angle, profile shift coefficients, and pressure angle

A final comparison was made to find the difference between the optimal solutions' power loss and mass, comparing "Case 0" and "Case 4". This comparison exhibits how close to the optimal solutions it is possible to reach when substituting design variables to fixed values. The selected values were, as previously, set to  $\beta = 25^\circ$ ,  $\alpha_n = 20^\circ$ , and  $x_{0,p} = 0, w = 0$ .



**Figure 3.9:** Increase in system power loss (left) and mass (right) when using fixed values for helix angle, profile shift coefficients, and pressure angle, instead of optimizing them.

Figure 3.9 shows that on average the optimized transmission can expect  $\sim 3\%$  higher power losses, and  $\sim 10\%$  greater mass, if the helix angle, profile shift coefficient, and pressure angle are not used as optimization variables. The 5th and 95th percentile are 1.50% and 5.40% for power loss difference, and 2.76% and 15.57% for mass difference.

### 3.3 Trade-off between optimization objectives

Figure 3.10 illustrates the trade-off between the optimization objectives, minimizing mass and power losses. The black dots represent different solutions to an optimized transmission layout. Solutions with low mass tend to have higher power losses, and vice versa.

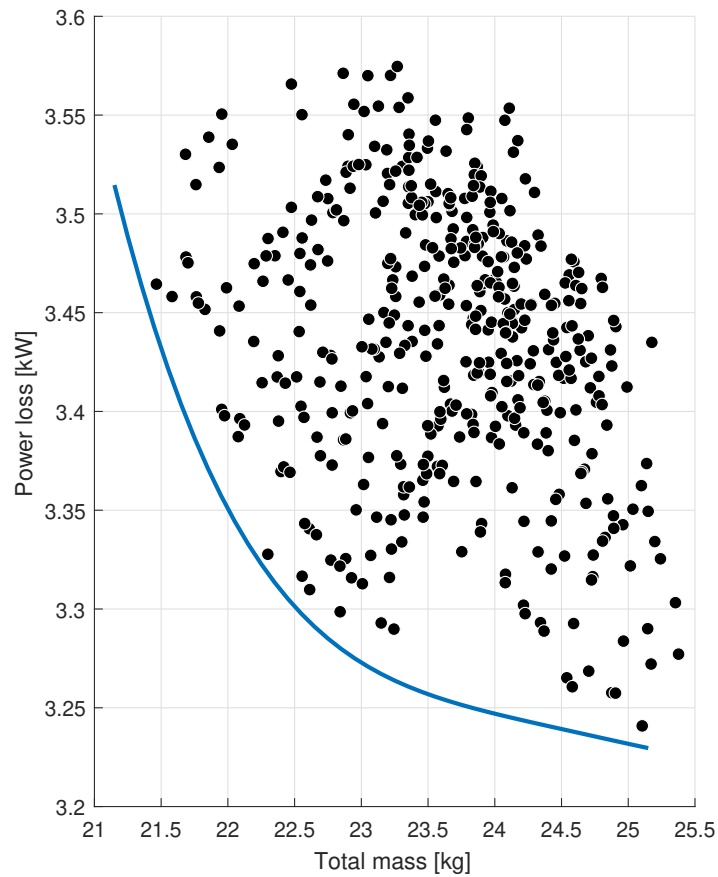


**Figure 3.10:** Mass and efficiency of system solutions. The trade-off between the objectives is clearly visualized by the plotted curve.

### 3.4 Running the finished transmission optimization tool

The transmission optimization tool was run for a two-stage layshaft transmission with the input data in Table 3.1.

**Table 3.1:** Input parameter values for testing transmission optimization tool for a two-speed two-stage layshaft transmission.

Parameter	Symbol	Input value
Desired gear ratio	$U$	8.28
Maximum input torque	$T_{max}$	582 Nm
Input torque @ KOP*	$T$	250 Nm
Rotational speed @ KOP*	$n$	8 400 rpm
Material density for gears	$\rho_{steel}$	7 800 kg/m <sup>3</sup>
Material density for shafts	$\rho_{steel}$	7 800 kg/m <sup>3</sup>
Material density for housing	$\rho_{Al}$	2 700 kg/m <sup>3</sup>

\*Key operating point, of the motor.

Outputs of the transmission optimization tool from the input data in Table 3.1, can be seen in Table 3.2 and in Figure 3.11. A graphical representation of the optimized transmission is seen in Figure 3.12.

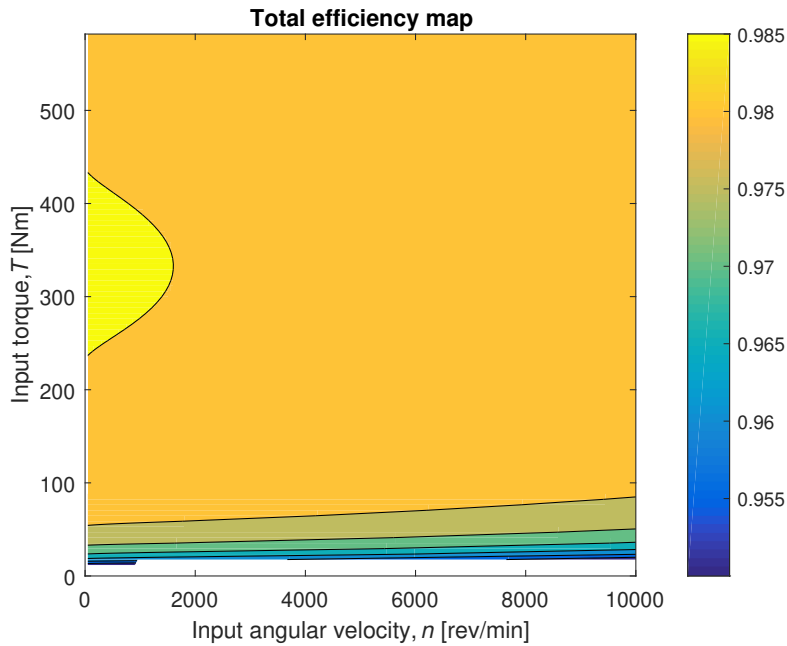


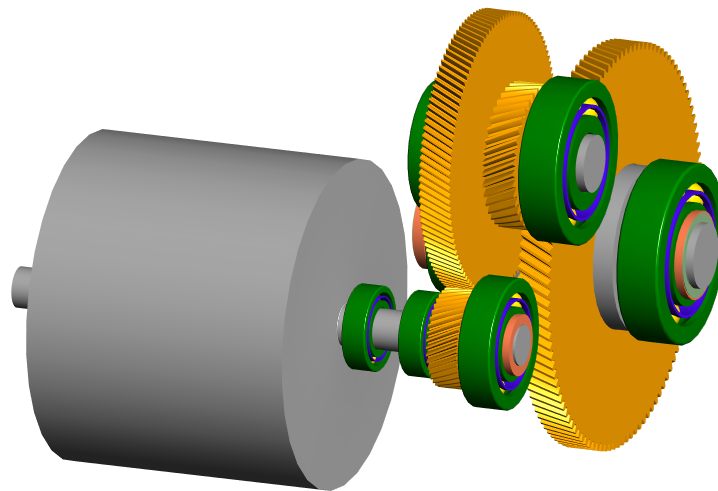
**Figure 3.11:** Graphical representation of efficiency map of the two-stage single-speed transmission, with input data from Table 3.1.

**Table 3.2:** Output values from testing transmission optimization tool for a single-speed two-stage layshaft transmission.

Parameter	Symbol	Output value
<i>General</i>		
Total system mass	$m$	26.4 kg
Actual gear ratio	$U$	8.265
System efficiency @ KOP	$\eta_P$	0.984
Transmission height	$H$	413.8 mm
Transmission length	$L$	369.8 mm
Transmission width	$W$	116.3 mm
<i>Gear stage 1</i>		
Gear ratio	$u_1$	2.878
Number of teeth on pinion	$z_{p,1}$	41
Number of teeth on wheel	$z_{w,1}$	118
Reference radius of pinion	$R_{p,1}$	28.27 mm
Reference radius of wheel	$R_{w,1}$	81.37 mm
Face width	$b_1$	21.25 mm
Normal module	$m_{n_1}$	1.250 mm
Normal pressure angle	$\alpha_{n_1}$	20°
Helix angle	$\beta_1$	25°
Profile shift coefficient of pinion	$x_{p_1}$	0
Profile shift coefficient of wheel	$x_{w_1}$	0
Dedendum	$h_{fP_1}$	1.563 mm
Addendum	$h_{aP_1}$	1.250 mm
Root radius	$\rho_{aP_1}$	0.438 mm
<i>Gear stage 2</i>		
Gear ratio	$u_2$	2.872
Number of teeth on pinion	$z_{p,2}$	39
Number of teeth on wheel	$z_{w,2}$	112
Reference radius of pinion	$R_{p,2}$	43.03 mm
Reference radius of wheel	$R_{w,2}$	123.6 mm
Face width	$b_2$	20.00 mm
Normal module	$m_{n_2}$	2.000 mm
Normal pressure angle	$\alpha_{n_2}$	20°
Helix angle	$\beta_2$	25°
Profile shift coefficient of pinion	$x_{p_2}$	0
Profile shift coefficient of wheel	$x_{w_2}$	0
Dedendum	$h_{fP_2}$	2.500 mm
Addendum	$h_{aP_2}$	2.000 mm
Root radius	$\rho_{aP_2}$	0.700 mm

**Table 3.2:** (continued)

Parameter	Symbol	Output value
<i>Input shaft</i>		
Shaft length	$l_{sh}$	77.25 mm
Shaft diameter	$d_{sh}$	25.00 mm
Bearing 1	-	SKF 6205 ETN9
Bearing 2	-	SKF 6405
<i>Mid shaft</i>		
Shaft length	$l_{sh}$	116.3 mm
Shaft diameter	$d_{sh}$	55.00 mm
Bearing 1	-	SKF 6207 ETN9
Bearing 2	-	SKF 6411
<i>Differential</i>		
Bearing 1	-	SKF 6309
Bearing 2	-	SKF 6410
<i>Gear mesh frequencies</i>		
GMFs	-	5 740, 1 897 Hz

**Figure 3.12:** Visual result of modeling optimization tool output parameters in MASTA, with input data from Table 3.1.

The transmission optimization tool was run for a two-speed two-stage layshaft transmission with the input data in Table 3.3.

**Table 3.3:** Input parameter values for testing transmission optimization tool for a two-speed two-stage layshaft transmission.

Parameter	Symbol	Input value
Desired gear ratios for each speed	$U_{1,2}$	15.6, 8.05
Maximum input torque	$T_{max}$	610 $Nm$
Input torque @ KOPs*	$T_{1,2}$	610, 250 $Nm$
Rotational speed @ KOPs*	$n_{1,2}$	5 000, 10 000 $rpm$
Material density for gears	$\rho_{steel}$	7 800 $kg/m^3$
Material density for shafts	$\rho_{steel}$	7 800 $kg/m^3$
Material density for housing	$\rho_{Al}$	2 700 $kg/m^3$

\*Key operating points, for each speed.

Some of the outputs of the transmission optimization tool from the input data in Table 3.3, can be seen in Table 3.4 and in Figure 3.13. A graphical representation of the optimized transmission is seen in Figure 3.14.

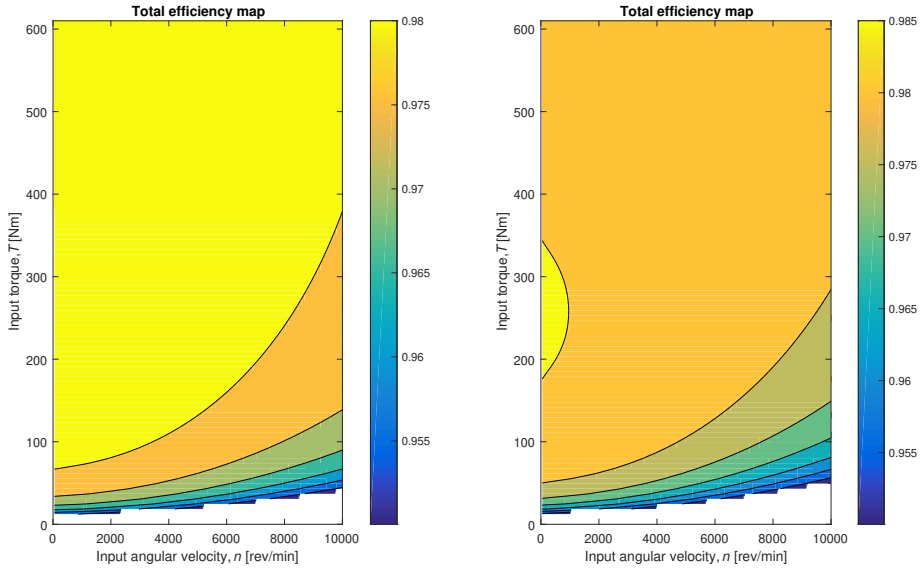


**Figure 3.13:** Graphical representation of efficiency map of the two-stage two-speed transmission, with input data from Table 3.3.

**Table 3.4:** Output values from testing transmission optimization tool for a two-speed two-stage layshaft

Parameter	Symbol	Output value
<i>General</i>		
Total system mass	$m$	54.3 kg
System efficiency @ KOPs	$\eta_{P_{1,2}}$	0.981, 0.979
Actual gear ratios	$U_{1,2}$	15.59, 8.21
Transmission height	$H$	548.4 mm
Transmission length	$L$	487.3 mm
Transmission width	$W$	160.0 mm
<i>Gear stage 1</i>		
Gear ratio	$u_{1,1,2}$	3.931, 2.070
Number of teeth on pinion	$z_{p,1,1,2}$	29, 57
Number of teeth on wheel	$z_{w,1,1,2}$	114, 118
Reference radius of pinion	$R_{p,1,1,2}$	31.20, 50.11 mm
Reference radius of wheel	$R_{w,1,1,2}$	122.6, 103.7 mm
Face width	$b_{1,1,2}$	19.50, 15.93 mm
Normal module	$m_{n_{1,1,2}}$	1.950, 1.593 mm
Normal pressure angle	$\alpha_{n_{1,1,2}}$	20°, 20°
Helix angle	$\beta_{1,1,2}$	25°, 25°
Profile shift coefficient of pinion	$x_{p_{1,1,2}}$	0, 0
Profile shift coefficient of wheel	$x_{w_{1,1,2}}$	0, 0
Dedendum	$h_{fP_{1,1,2}}$	2.438, 1.992 mm
Addendum	$h_{aP_{1,1,2}}$	1.950, 1.593 mm
Root radius	$\rho_{aP_{1,1,2}}$	0.683, 0.558 mm
<i>Gear stage 2</i>		
Gear ratio	$u_2$	3.967
Number of teeth on pinion	$z_{p,2}$	30
Number of teeth on wheel	$z_{w,2}$	119
Reference radius of pinion	$R_{p,2}$	41.38 mm
Reference radius of wheel	$R_{w,2}$	164.1 mm
Face width	$b_2$	27.50 mm
Normal module	$m_{n_2}$	2.500 mm
Normal pressure angle	$\alpha_{n_2}$	20°
Helix angle	$\beta_2$	25°
Profile shift coefficient of pinion	$x_{p_2}$	0
Profile shift coefficient of wheel	$x_{w_2}$	0
Dedendum	$h_{fP_2}$	3.125 mm
Addendum	$h_{aP_2}$	2.500 mm
Root radius	$\rho_{aP_2}$	0.875 mm

**Table 3.4:** (continued)

Parameter	Symbol	Output value
<i>Input shaft bearings</i>		
Shaft length	$l_{sh}$	108.4 mm
Shaft diameter	$d_{sh}$	25.00 mm
Bearing 1	-	SKF 6005
Bearing 2	-	SKF 6405
<i>Mid shaft bearings</i>		
Shaft length	$l_{sh}$	159.9 mm
Shaft diameter	$d_{sh}$	50.00 mm
Bearing 1	-	SKF 6307
Bearing 2	-	SKF 6410
<i>Output shaft bearings</i>		
Bearing 1	-	SKF 6411
Bearing 2	-	SKF 6412
<i>Gear mesh frequencies</i>		
GMFs (speed 1)	-	2 417, 636 Hz
GMFs (speed 2)	-	4 750, 1 208 Hz

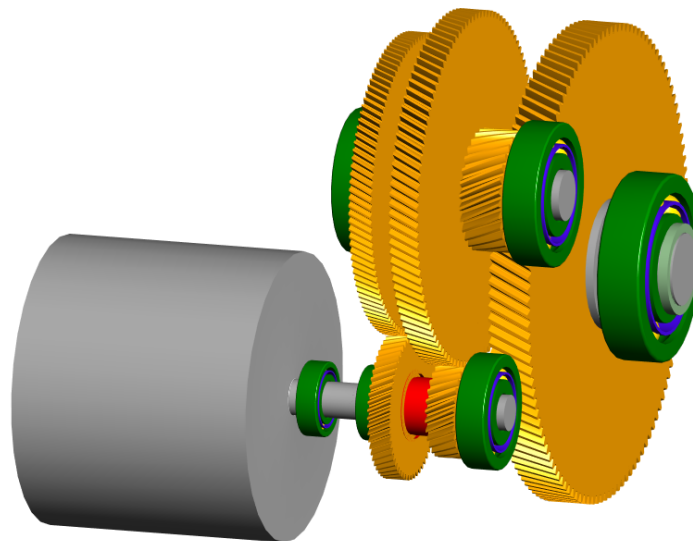


**Figure 3.14:** Visual result of modeling optimization tool output parameters in MASTA. A two-speed two-stage layshaft transmission defined by parameters in Table 3.3.



## 4 Discussion

### 4.1 Evaluation of results

One of the main aspects differentiating the work conducted in this master thesis to similar studies have been the addition of a target for execution time. The optimization tool consists of component and efficiency models that allow for a high level of detail, since there were a large number of design variables which could be varied. However, using the full level of detail resulted in execution times which were far beyond the target.

There is a clear trend in all results of execution time indicating an increase depending on the amounts of speeds. It is not surprising, since the more speeds there are the more gears need to be optimized. As the gears are the components with the most intricate models, it takes notably longer time to optimize layouts with more gears. Another reason for multi-speed transmissions taking longer time to optimize is the fact that the power loss maps are generated for each speed of the transmission.

From Figure 3.1, it is evidently necessary to use fixed parameter values to reach the target for optimization time. When running the optimization transmission tool at its fullest potential, i.e. "Case 0", the execution time was around 30 seconds. Using a fixed value for the helix angle was therefore evaluated in "Case 1". Since the helix angle was chosen as the optimization variable for the system optimization, there was only one system solution when keeping the helix angle fixed, which resulted in execution times below one second for "Case 1". However, Figure 3.6 shows an increase in both power loss and mass for the optimized solutions, when comparing "Case 1" with "Case 0". From the results in Section 3.2.1 it is apparent that assigning a fixed value for the helix angle ( $\beta = 25^\circ$ ), leads to solutions presented by the transmission optimization tool having higher power losses ( $\sim 2 \pm 2\%$ ), and significantly higher mass ( $\sim 9 \pm 5\%$ ).

The differences in optimization results for comparing "Case 1" with "Case 2" and "Case 3", were not as significant as the comparison between "Case 0" and "Case 1". Comparisons show that the impact of fixing profile shift coefficients and pressure angle does not compromise the overall results to the same extent, when already using a fixed value for the helix angle. A fixed value for profile shift coefficients has a slightly larger impact on optimization results than when using a fixed value for pressure angle. This is likely due to the fixed profile shift coefficients affecting two design parameters,  $x_{0,p}$  and  $x_{0,w}$ . Further, Miler et al. [33] found that gears optimized with profile shift had significantly lower power loss and a smaller volume, for their optimization with the objectives to minimize volume and power loss of spur gears. Their conclusions correlates with the findings of this thesis.

The final evaluation, made in Section 3.2.4, exhibits the difference between the optimal solution presented by the highest possible level of detail of the transmission optimization tool (Case 0) and its counterpart when assigning fixed values to four of the design variables (Case 4). As Figure 3.9 shows, at least 9 out of 10 solutions had a difference in power loss between 1% and 6%, and a difference in mass between 2% and 16%. The variety in power loss and mass difference can be explained by the scoring model.

The implemented scoring model slightly favors higher efficiency over a lower mass in the trade-off between the objectives, illustrated in Figure 3.10. However, it is important to note that this does not mean that the scoring model is insufficient or biased. The scoring model's purpose is to translate the two optimization objectives, minimizing power loss and mass, to a single metric which can be used to compare different solutions. The scoring model was designed to compare the effects of power loss and mass on the overall power consumption of the vehicle, and as it seems decreasing power loss reduces power consumption more efficiently than lowering mass does. However, the scoring model was developed to only take the mass' effect on power consumption in to account, but there may be other disadvantages of increasing mass, which are further discussed in Section 4.2.

For some samples in the histogram the difference, between the optimal solutions with varying versus fixed design variables, was negative. A negative difference implies that the solution with fixed design parameter was an improvement. However, if the fixed parameter solution had decreased power losses, it would have an increase in mass, in accordance with the trade-off in Figure 3.10. Meaning, that the total score of a solution with fixed variables would never have a higher total score than a solution with fewer fixed variables.

## 4.2 Discussing the scoring model

### 4.2.1 Mass' impact on power consumption

The scoring model translates the mass of the transmission into power consumption of the vehicle, seen in Equation 33. It is done by calculating the power needed to overcome the increased rolling resistance from the increased mass of the vehicle. In Section 2.6 an example of how much one additional kilogram of mass impacts the power consumption of a certain vehicle. It is important to note that the factor presented in Equation 34,  $\eta_m = 0.9998$  per kg, is highly dependent on the vehicle itself. If the vehicle is heavier to begin with, an addition kilogram will entail a smaller percentage increase, thus a smaller impact on the power consumption. Further, the mass power consumption equation includes a term for drag loss, which is impacted by the geometry of the vehicle. Because of these reasons, the scoring model is updated with new input data depending on the vehicle application of the optimized transmission.

Another factor impacting the result of the scoring model is the drive cycle of the vehicle. The current scoring model calculates power consumption at a constant speed. Vehicle applications with a varied drive cycle may not be properly represented, when using a constant speed in the scoring model.

### 4.2.2 Trade-off in reference literature

The trade-off between optimization objectives, seen in Figure 3.10, is not unusual in optimization of transmission systems and components. Kim et al. [7] found a trade-off in mass and efficiency, when optimizing a gearbox with helical gears with mass and efficiency as optimization objectives. Patil et al. [8] optimized a two-stage helical gearbox, with the objectives to minimize volume and power loss. They found a trade-off between low power loss and small volume of the transmission. Miler et al. [33] did a similar study as Patil et al. [8], and found a pareto front for the solutions. A conflict in optimization objectives was presented in this thesis as a trade-off between low mass and low power loss, which was also found in the literature.

### 4.2.3 Weighting of objectives

When selecting an optimal solution, the scoring model compares the two optimization objectives over their influence of power consumption. The power consumption comparison was made in order to ensure that the optimization objectives were compared without bias. However, in certain applications there may be an interest to alter what the scoring model should consider as optimal. For instance, if a vehicle manufacturer wants to create a vehicle with minimized mass of the transmission, and high efficiency is not as crucial.

The impact of prioritization of optimization objectives is outlined by the comparisons in Figure 4.1, where different weighting of the scoring objectives are used. Equation 38 is a modified scoring model equation with an additional weight factor,  $k$ , to manually change the priority between the objectives.

$$\text{score} = k \cdot \eta_P + (1 - k) \cdot \eta_m \quad (38)$$

Figure 4.1 illustrates three different transmission systems with the same input parameters, but with varying weight factors in the modified scoring model in Equation 38.

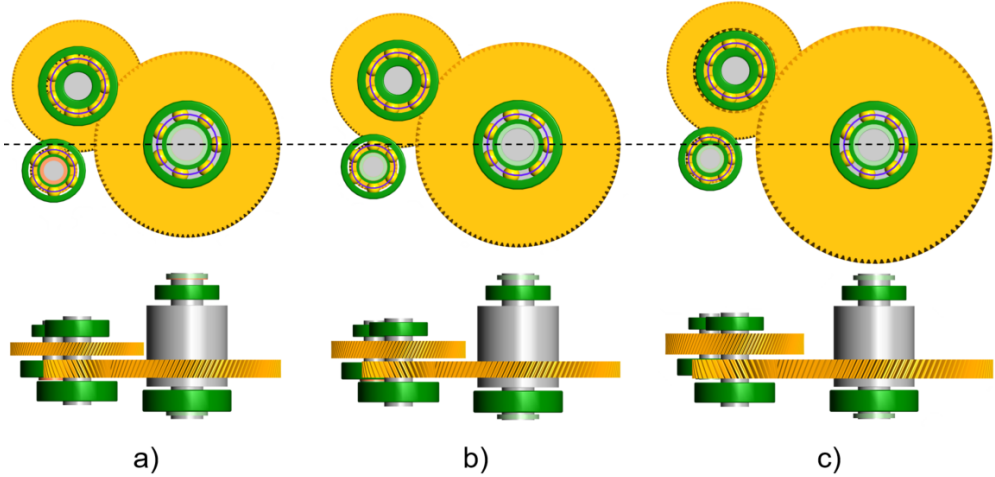


**Figure 4.1:** Transmission systems with the same input parameters, but with different weighting factor for objectives, according to Table 4.1

With an increased  $k$ , i.e. prioritization of  $\eta_P$ , particularly gears in the second gear stage increases in diameter. The face width of the gears also increase with an increased  $k$ . Consequently, as Table 4.1 shows, the mass increases with more than 40% when going from  $k = 0.25$  to  $k = 0.75$ . The efficiency increased 0.15 percentage points for the same change in weighting.

**Table 4.1:** Data for transmission systems in Figure 4.1.

Parameter	a)	b)	c)
Weighting factor, $k$	0.25	0.50	0.75
System mass	24.76 kg	26.68 kg	35.30 kg
System efficiency	98.39%	98.44%	98.54%

The comparison between different weighting factors shows the impact of specifying the trade-off between optimization objectives. It is important to note that the transmission systems in Figure 4.1 are all optimal solutions, and that no specific one is better than the others. However, the comparison highlights the importance of understanding the trade-off between the objectives, where an inappropriate weighting can result in undesirable solutions.

#### 4.2.4 Volume as a scoring objectives

The effect of increased mass of the transmission systems regarding the score is purely from a power consumption point of view. Other implications of increased mass, such as a potential increase in manufacturing costs and material costs are not considered in the scoring model, as costs were outside the scope of the thesis. There may also be other factors that are necessary to take into consideration when scoring transmission systems.

With increased mass the volume of the transmission is likely to increase. Larger volume means taking up more space in the chassis, which could reduce the available space for the battery pack in an electric vehicle. Consequently, the reduced battery size will lead to an energy capacity reduction for the vehicle. Equation 39 is used to calculate the energy reduction factor as a result of the transmission system's volume by multiplying it with the battery's energy density, and subsequently subtracting from the batteries total energy capacity.

$$\eta_V = \frac{E_{bat} - Vu_{bat}}{E_{bat}} \quad (39)$$

With assumed values for the energy density of batteries  $u_{bat} = 400 \text{ kWh}/\text{m}^3$ , the battery's energy capacity  $E_{bat} = 75 \text{ kWh}$ , and the transmissions volume  $V = 0.4 \cdot 0.2 \cdot 0.1 = 0.008 \text{ m}^3$ :

$$\eta_V = \frac{75 - 0.008 \cdot 400}{75} = 0.96 \quad (40)$$

The example in Equation 40 demonstrates that the transmission system's volume lowers the vehicle's energy capacity with a factor 0.96, which can be compared with the efficiency factor,  $\eta_P$ , and the mass power loss factor,  $\eta_m$ . Inclusion of  $\eta_V$  changes the scoring (Equation 35) to:

$$\text{score} = \eta_P \cdot \eta_m \cdot \eta_V \quad (41)$$

A comparison between the optimal solutions of a transmission system based on excluding or including the influence of increased volume is presented in Table 4.2.

**Table 4.2:** Transmission mass and efficiency of optimal solutions depending on excluding or including the transmission's volume in the scoring model (input data from Table 3.1).

Parameter	Excluding $\eta_V$	Including $\eta_V$
System mass	22.85 kg	18.22 kg
System efficiency	98.50%	98.35%

In Table 4.2 the difference in mass and efficiency of the optimized transmissions can be seen. The system mass is lower for the solution where  $\eta_V$  was included, since the scoring model had an increased motive to minimize volume which correlates with mass. In other words, the trade-off between minimizing mass and maximizing efficiency has shifted further towards minimizing mass. Consequently, the efficiency of the optimal solution has decreased when including the volume's effect on the score, since the scoring model does not value maximizing efficiency to the same extent. This signifies the importance of the scoring model's accuracy in terms of prioritization of objectives, where as many and as realistic implications of increased mass and power losses are taken in to consideration. However, certain factors are difficult to model. The reason for not including  $\eta_V$  in the actual scoring model, is the lack of input parameters regarding the battery. As the battery is outside the scope of the project there is no known data for utilizing Equation 39. It is also likely that the assumption, that the entire volume of the transmissions would be occupied by batteries, is not always a fact.

## 4.3 Optimization methods

### 4.3.1 Gear-set optimization

The iterative gear-set optimization method was able to reduce the number of calculations. However, a point of interest is if the result of the optimization process is the actual top solution. There is a chance that the iteration based process will miss the optimal solution if there are several close contenders. This is explained in Figure 4.2.

The number of calculated gear-sets in each iteration depends on the total number of iterations. Fewer iterations leads to more calculations, where the extreme of one iteration results in calculation of the entire population.

More iterations entails fewer calculations in each iteration, as the "step length" between calculated solutions increases with the number of iterations. Figure 4.2 illustrates a data set which is sampled with two different "step lengths" between the sample points ( $L_{step} = 3$  and  $L_{step} = 4$ ). The data sets clearly has two peaks, where the right peak contains the highest point, i.e. top overall solution. When sampling with  $L_{step} = 3$  the identified top solution is the actual top

solution, which is as intended. However, with  $L_{step} = 4$  the actual top solution was missed since it is between two sample points. Instead the second peak is identified as the top solution, and the actual top solution has been overlooked.

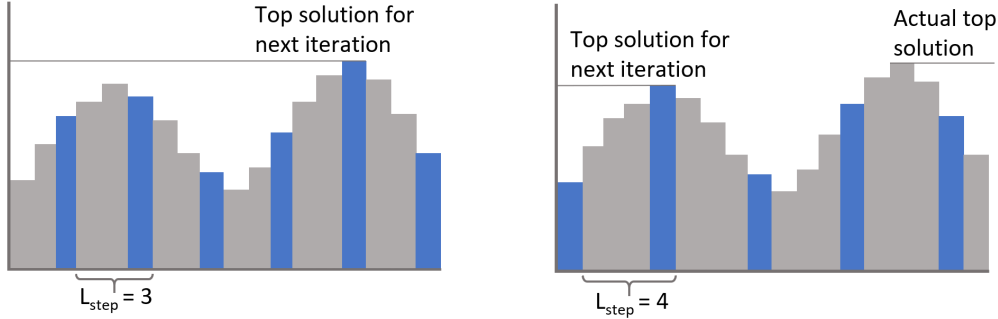


**Figure 4.2:** Determination of top solution of a data set, dependent on distance between sample points,  $L_{step}$ . The colored bars represent the sampling points.

To summarize, an increased number of iterations leads to fewer calculations, resulting in lower execution time. As a trade-off, the risk of missing an optimal solution increases, as the "step length" increases with more iterations. Table 4.3 shows execution time and deviation from optimal solution based on the number of iterations.

**Table 4.3:** Number of iterations for gear mesh optimization, and how it affects execution time and deviation from the score when using one iteration.

No. of iterations	Deviation in score from N=1	Execution time
N = 1	–	~ 31 ms
N = 2	0.01%	~ 12 ms
N = 3	0.09%	~ 6 ms
N = 4	0.16%	~ 5 ms
N = 5	0.56%	~ 5 ms

As Table 4.3 shows, the deviation in score from optimizing with  $N = 1$  increases with the number of iterations. As for execution time, there is a significant drop when going from one to three iterations. However, with four or five iterations the execution time stagnates, while the deviation in score continues to increase. With this in mind, three iterations were used for the gear-set optimization.

In Table 2.4 it can be seen that the ranges of the design parameters have different lengths. For instance, the  $m_n$ -range contains 51 values, whereas the  $\alpha_n$ -range contains 11 values. The final ranges were determined after experimenting with different ranges and seeing how it impacted the spread of solutions, where it was desired to have many viable solutions that could be compared. The iteration based optimization process has no trouble dealing with the different lengths of parameter ranges, since it will adapt each interval depending on the length of range for that variable.

### 4.3.2 System optimization

Transmission systems consist of several different components, which affect not only the system performance but also possibly constrains other components' design. As a pair of helical gears meshes, axial forces are generated as the angled flanks come in contact. Axial mesh forces result in axial loads on the bearings, which is least favorable for the deep groove ball bearings used in

the bearing model. Hence, the helix angle was used as the optimization parameter in the system optimization, even though other gear parameters affect the system forces.

As discussed in Section 4.1 "Evaluation of results", the helix angle dependent system optimization lead to execution times far above the target, when optimizing a two-stage layshaft transmission. Not only gear-sets, but all other components and their respective power losses, needed to be calculated for every combination of helix angles, which resulted in a substantial increase in number of calculations. Further, a three-stage layshaft transmission would have even longer execution time, since yet another helix angle would have to be varied.

Because of the issues with execution time, the helix angle dependent system optimization is not used in the finished transmission optimization tool. Ultimately, it was the combination of the system optimization and the level of detail of the component models that resulted in the extensive execution time. A lowered level of detail in the component models could maybe make the system optimization viable, but the optimization results would be compromised by the reduced level of detail.

### 4.3.3 Alternative method for optimization

An alternative method for system optimization considered in this thesis was using pre-calculated values for gear-sets. The idea was to calculate the optimal gears ahead of time and store the solutions in a database. The gear models could then be collected from the database in a fraction of the time it took to optimize them.

The idea was based around the system optimization discussed in Section 2.7.2 "System optimization", where gears modeled from different combinations of gear ratio, torque, speed, and helix angles were selected from the database based on the input parameters for the transmission system being optimized. This entailed that gear-sets defined by every combination of the four mentioned variables needed to be optimized ahead of time. For every combination only one solution was saved in the pre-calculated gear-sets database.

It could take several hours to optimize all the gear-sets, and save them to the database. However, since the time to execute the live system optimization was heavily reduced thanks to the short time to collect the gear-set solutions from the database, it seemed like this could be a viable strategy when optimizing a large amount of transmission systems.

The shortfall of the strategy of using pre-calculated gear-sets came when incorporating the multi-speed transmission layouts. In a multi-speed transmission all parallel gear-sets need to operate with the same center distance. Since the pre-calculated gear-sets were only optimized based on gear ratio, torque, speed, and helix angle, the center distance could vary freely for the optimal solutions. Technically, it would be possible to add center distance to the list of variables defining the pre-calculated gear-sets, but it would entail further increasing the time to optimize gear-sets for all combinations of the mentioned variables. The gear-sets need to be optimized before each run of the entire electric power train optimization tool, since prerequisites for the scoring model are different depending on the vehicle being optimized. Thus, the pre-calculation procedure would likely be too time consuming with the addition of predetermined center distances.

## 4.4 MATLAB

MATLAB was the software program used for the optimization tool. To be able to decrease the execution time for the tool, arrays were utilized as much as possible since MATLAB use arrays to execute several calculations concurrently. Execution time will vary depending on how many cores the computer running the optimization has, since the number of cores determine how many calculations can be performed in parallel [36]. The iteration based gear-set optimization decreases the number of calculations that need to be performed in parallel, and is therefore more crucial for computers with fewer cores. It may therefore be necessary to re-evaluate the number

of iterations used in the gear-set optimization process, depending on the specifications of the computer running the optimization.

The execution time also varied from run to run of one optimized solution, which likely depends on background processes on the computer which share computational resources.

## 4.5 Sizing and efficiency models

### 4.5.1 Gear sizing model

The ISO 6336 standard is widely used for gear sizing in automotive industry, and provides the gear sizing model in this thesis with credibility, as it has been validated for the values of design variables used.

The gear design variables used in the gear sizing model were selected based on referenced literature. Patil et al. [8] optimize a helical gear-set based on varying normal module, number of teeth, face width, and helix angle. Kim et al. [7] adds normal pressure angle as an addition to the variables used by Patil et al. [8]. According to Miler et al. [33], solutions with profile shift both had lower volume and decreased power losses, therefore profile shift was set as supplementary design variable in this thesis.

### 4.5.2 Comparison of oil seal loss equations

The oil seal power loss equations in Table 4.4 were compared against power loss data provided by BorgWarner. The equation by Linke [27] was selected, since it was the closest match with the power loss data.

**Table 4.4:** Seal power loss equations considered in this thesis.

Reference	Input variables	Comment
ISO/TR 14179-1 [26]	$d_{sh}, n$	Only two types of seals taken into consideration.
Linke [27]	$d_{sh}, n, \theta, \nu$	Closest match with seal power loss data.
Freudenberg Simrit [27]	$d_{sh}, n$	Based on one type of oil.

$d_{sh}$  is shaft diameter,  $n$  is rotational speed,  $\theta$  is temperature,  $\nu$  is oil viscosity.

### 4.5.3 Model validation

Validation of efficiency models was done by comparing modeled data with test data, test data which is confidential property of BorgWarner, from a specific transmission system. However, as the testing results from BorgWarner only corresponded to the combined losses of the entire transmission system, it was not possible to validate the separate efficiency models of different components.

A comparison of the total non-loaded losses concluded that the transmissions modeled in this thesis had similar non-loaded losses as the test data.

## 4.6 Objectives and limitations

The objective to create a tool for optimizing mechanical transmissions within the target execution time has been fulfilled. In terms of describing the trade-offs in optimization of mechanical transmissions, the discussion in Section 4.2 "Discussing the scoring model" covers the key findings. As found, there is a trade-off between low mass and low power losses, when combing the objectives in the scoring model. Priority in the objective trade-off is determined by the equations

used for combining the objectives into a score, which is why it is important to create accurate conversions for mass and power losses to the combined score metric.

Effects of limitations listed in Section 1.4, are discussed below.

1. Cost of transmissions was outside the scope of this thesis. It is possible that the optimal transmission solution will be different when considering cost. However, implementation of cost models are likely to work well in combination with the current scoring model, where costs would be compared with mass and efficiency.
2. A static load case was assumed for sizing of components, thus effects of dynamics and fatigue on components were not considered. The reason behind the selection of a static load case was due to unknown load cycles from the motor. The proposed optimal transmission system would have to be validated for an actual load case, if further development is made from a suggested transmission system.
3. The differential was modeled as a solid shaft with a fixed mass independent of load or size of other components, and power losses from inside the differential were not considered. Transmission systems with different loads may be affected variously by not having a realistic model of the differential.
4. Shifting elements and other components linked solely with multi-speed transmissions were not modeled. This might cause injustice when comparing single-speed and multi-speed transmissions, since the impact of additional mass and power losses of shifting components are not considered for the multi-speed transmissions.
5. Optimal transmission solutions of this thesis only regard layshaft transmissions, which leads to the possibility that other transmission layouts, e.g. planetary transmissions, could be more optimal in certain situations.

## 4.7 Further work

### 4.7.1 System dynamics

Dynamic effects, such as noise, vibration, and harshness (NVH) may be relevant to consider when optimizing transmissions for electric powertrains.

Because of the low noise from the electric motor, noise from the mechanical transmission is more profound in EVs than in vehicles with an internal combustion engine. The peak-to-peak static transmission error (PPSTE) is linked with the vibrations of the gears, resulting in noise [7]. Kim et al. [7] find that PPSTE can have a substantial impact when used as an optimization objective, which proposes that the transmission error could be important to consider in further development of the transmission optimization tool.

### 4.7.2 Detailed analysis of fixed values for design variables

The finished optimization tool utilizes fixed values for design variables in order to reach the target for execution time. However, the fixed values were assigned as constant, independent of input torque, gear ratio, or any other parameter. It may be possible to assign fixed values based on, for example, the torque level to get an improved optimization result. Multi-speed and three-stage layouts could be subject to the same investigation.

The reason for not further investigating the fixed values in this thesis was because of a lack of time at the end of the project.

### 4.7.3 Planetary transmissions

The implementation of a model for planetary gear-sets have been started, but results are not verified. By implementing more transmission layouts, comparisons between the different layouts



can be performed to gain further insight in optimization of mechanical transmissions for electric powertrains.

## 5 Conclusion

- I. For the finished optimization tool four design variables were fixed, referenced as "Case 4", in order to reach the target for execution time. "Case 4", with the fixed values  $\beta = 25^\circ$ ,  $\alpha_n = 20^\circ$ , and  $x_{0,p} = x_{0,w} = 0$ , was compared with "Case 0" where all design variables were varied.

The optimal transmission solutions of "Case 4" had a 1.5% to 5.4% increase in power loss, and a 2.76% to 15.57% increase in mass compared to the optimal solutions in "Case 0". The differences highlighted that the number of design variables had a clear influence on the quality of the optimized solutions.

Fixing variables (Case 4) resulted in an execution time decrease, from  $\sim 25$  s to  $\sim 29$  ms for a two-stage single-speed transmission, from  $\sim 26$  s to  $\sim 51$  ms for a two-stage two-speed transmission, and from  $\sim 30$  s to  $\sim 81$  ms for a two-stage three-speed transmission. Thus, the target for execution time was met and *RQ3* has been answered.

- II. Gear-set optimization was based on iterations, where the number of iterations affected accuracy and execution time. When iterating in three steps,  $N = 3$ , the execution time was reduced from  $\sim 31$  ms to  $\sim 6$  ms per gear-set, and the score of the optimal solution decreased by 0.09% relative to  $N = 1$  iteration.
- III. Prioritization of the two scoring objectives was discussed in Section 4.2 "Discussing the scoring model". It became apparent that with increased priority on minimizing power loss, the mass of the transmission could increase up to 40%. This signified the trade-off in optimization of mechanical transmissions, the mass will increase when aiming towards increased efficiency, which has answered *RQ2*.

If it is assumed that an increased volume of the transmission reduces the available space for the battery pack, another trade-off occurs. In this case there is a compromise between increasing energy capacity, i.e. having a larger battery, and increasing the vehicle's efficiency, resulting in a larger transmission. When using volume as an objective to rank the solutions, the mass of the optimal transmission would decrease from 22.85 kg to 18.22 kg, and the system efficiency decrease from 98.50% to 98.35%.

The final conclusion of this thesis, and the answer to *RQ1*, is that the detail of component models and the compromise between optimization objectives, have an important role in attaining the most optimal transmission design.

# References

1. IEA. Global stock of electric cars , 2010-2020. International Energy Agency. 2021. Available from: <https://www.iea.org/data-and-statistics/charts/global-electric-passenger-car-stock-2010-2020> [Accessed on: 2021 Jun 1]
2. IEA. Global EV Outlook 2020. International Energy Agency. 2020. Available from: <https://www.iea.org/reports/global-ev-outlook-2020> [Accessed on: 2021 Feb 15]
3. IEA. Tracking Transport 2020. International Energy Agency. 2020. Available from: <https://www.iea.org/reports/tracking-transport-2020> [Accessed on: 2021 Jun 1]
4. Michaelis K, Höhn B, and Hinterstoißer M. Influence factors on gearbox power loss. *Industrial Lubrication and Tribology*, 2011 2011; 63:46–55
5. Domingues-Olavarría G. Modeling, Optimization and Analysis of Electromobility Systems. Department of Biomedical Engineering, Lund university. PhD thesis. 2018
6. Domingues-Olavarría G, Márquez-Fernández F, Fyhr P, Reinap A, Andersson M, and Alakula M. Optimization of Electric Powertrains Based on Scalable Cost and Performance Models. *IEEE Transactions on Industry Applications* 2019; 55
7. Kim Sc, Moon Sg, Sohn Jh, Park Yj, Choi Ch, and Lee Gh. Macro geometry optimization of a helical gear pair for mass, efficiency, and transmission error. *Mechanism and Machine Theory* 2020; 144
8. Patil M, Ramkumar P, and Shankar K. Multi-objective optimization of the two-stage helical gearbox with tribological constraints. *Mechanism and Machine Theory* 2019; 138:38–57
9. Mendi F, Boran K, Başkal T, and Boran F. Optimization of module, shaft diameter and rolling bearing for spur gear through genetic algorithm. *Expert Systems with Applications* 2010; 37:8058–64
10. Domingues-Olavarría G, Márquez-Fernández FJ, Fyhr P, Reinap A, Andersson M, and Alakula M. Scalable performance, efficiency and thermal models for electric drive components used in powertrain simulation and optimization. 2017 :644–9
11. Fyhr P, Domingues-Olavarría G, Reinap A, Andersson M, and Alakula M. Performance and manufacturability tradeoffs of different electrical machine designs. 2017
12. Kollmeyer P, McFarland J, and Jahns T. Comparison of class 2a truck electric vehicle drivetrain losses for single- and two-speed gearbox systems with IPM traction machines. 2015
13. Roozegar M, Setiawan Y, and Angeles J. Design, modelling and estimation of a novel modular multi-speed transmission system for electric vehicles. *Mechatronics* 2017; 45:119–29
14. Han K, Wang Y, Filev D, Dai E, Kolmanovsky I, and Girard A. Optimized Design of Multi-Speed Transmissions for Battery Electric Vehicles. 2019 :816–21
15. Damiano A, Floris A, Marongiu I, Porru M, and Serpi A. Efficiency assessment of Electric Propulsion Systems for electric vehicles. *2016 International Symposium on Power Electronics, Electrical Drives, Automation and Motion (SPEEDAM)*. 2016 :1232–7
16. Vu N. A new study on the optimal prediction of partial transmission ratios of three-step helical gearboxes with second-step double gear-set. *WSEAS TRANSACTIONS on APPLIED and THEORETICAL MECHANICS* 2007; 2:229–38
17. Lecinski P. GMF calculation and gearbox problems detection. 2020 Oct
18. ISO. ISO 6336-1:2019(E). Calculation of load capacity of spur and helical gears - Part 1: Basic principles, introduction and general influence factors. International Standard, 2019
19. ISO. ISO 6336-2:2019(E). Calculation of load capacity of spur and helical gears - Part 2: Calculation of surface durability(pitting). International Standard, 2019
20. ISO. ISO 6336-3:2019(E). Calculation of load capacity of spur and helical gears - Part 3: Calculation of tooth bending strength. International Standard, 2019
21. Dudley DW. Handbook of practical gear design. Technomic Publishing, 2002
22. ANSI/AGMA. ANSI/AGMA 6001-D97. Design and selection of components for enclosed gear drives. The American Gear Manufacturers Association, 1997
23. Group S. SKF General Catalogue 5000. 2003 :49–85

24. Schlegel C and Hösl A. Detailed Loss Modelling of Vehicle Gearboxes. 2009 Oct
25. Bogdan C and Zoltan-Iosif K. Efficiency Investigation on a Helical Gear Transmission. *Analele Universității "Eftimie Murgu" Reșița: Fascicola I, Inginerie* 2017; XXIV:55–66
26. ISO. ISO/TR 14179-1:2001(E). Gears - Thermal capacity - Part 1: Rating gear drives with thermal equilibrium at 95 °C sump temperature. International Standard, 2001
27. Fernandes C. Power loss in rolling bearings and gears lubricated with wind turbine gear oils. PhD thesis. 2015
28. ISO. ISO/TR 14179-2:2001(E). Gears - Thermal capacity - Part 2: Thermal load-carrying capacity. International Standard, 2001
29. Wikipedia. Automobile drag coefficient. 2021. Available from: [https://en.wikipedia.org/wiki/Automobile\\_drag\\_coefficient](https://en.wikipedia.org/wiki/Automobile_drag_coefficient) [Accessed on: 2021 Jun 10]
30. Wargula Ł, Wieczorek B, and Kukla M. The determination of the rolling resistance coefficient of objects equipped with the wheels and suspension system – results of preliminary tests. *MATEC Web of Conferences 254, 01005 (2019)*. 2018
31. Tesla. Tesla Model 3. 2021. Available from: [https://www.tesla.com/sv\\_se/model3](https://www.tesla.com/sv_se/model3) [Accessed on: 2021 May 24]
32. ISO. ISO 53:1998. Cylindrical gears for general and heavy engineering - Standard basic rack tooth profile. International Standard, 1998
33. Miler D, Žeželj D, Lončar A, and Vučković K. Multi-objective spur gear pair optimization focused on volume and efficiency. *Mechanism and Machine Theory* 2018 :185–95
34. Samya B, Kaoutar D, El Mostapha B, Aziz B, and Samira E. A Multiobjective Optimization Analysis of Spur Gear Pair: The Profile Shift Factor Effect on Structure Design and Efficiency. *Mathematical Problems in Engineering* 2021; 2021
35. Rai P, Agrawal A, Saini ML, Jodder C, and Barman AG. Volume optimization of helical gear with profile shift using real coded genetic algorithm. *Procedia Computer Science* 2018; 133:718–24
36. MathWorks. MATLAB Multicore. Available from: <https://www.mathworks.com/discovery/matlab-multicore.html> [Accessed on: 2021 Jun 14]
37. ISO. ISO 6336-5:2019(E). Calculation of load capacity of spur and helical gears - Part 5: Strength and quality of materials. International Standard, 2016

# A Appendix

## A.1 Parameter values

**Table A.1:** Summary of factors for sizing of involute gears according to ISO 6336 [18]. Factors without a specified value are calculated in the models.

Influence factor	Value	Motivation
<i>Load factors</i>		
Application factor, $K_A$	1.0	Smooth running conditions assumed.
Mesh load factor, $K_\gamma$	1.0	Assumed that all load path share the common load equally.
Internal dynamic factor, $K_V$	–	
Face load factors, $K_{H\beta/F\beta}$	–	
Transverse load factors, $K_{H\alpha/F\alpha}$	–	
<i>Contact factors</i>		
Contact factor (pinion), $Z_B$	1.0	Suitable geometrical modifications can be achieved for final design.
Contact factor (wheel), $Z_D$	1.0	Suitable geometrical modifications can be achieved for final design.
Zone factor, $Z_H$	–	
Elasticity factor, $Z_E$	–	
Contact ratio factor, $Z_\epsilon$	–	
Helix angle factor, $Z_\beta$	–	High accuracy and optimum tooth flank modifications assumed.
Life factor (reference), $Z_{NT}$	1.6	Static load case assumed, according to MASTA.
Lubricant factor, $Z_L$	–	
Velocity factor, $Z_V$	–	
Roughness factor, $Z_R$	–	
Work hardening factor, $Z_W$	–	
Size factor (pitting), $Z_X$	2.0	According to ISO [37].
<i>Bending factors</i>		
Form factor, $Y_F$	–	
Stress correction factor, $Y_S$	–	
Helix angle factor, $Y_\beta$	–	
Rim thickness factor, $Y_B$	1.0	Rim sufficiently thick to withstand failure through fatigue.
Deep tooth factor, $Y_{DT}$	1.0	ISO Tolerance Class $> 4$ for all gears.
Stress correction of test gears, $Y_{ST}$	2.0	According to ISO [37].

**Table A.1:** (continued)

Influence factor	Value	Motivation
Life factor, $Y_{NT}$	2.5	Static load case assumed.
Relative notch sensitivity factor, $Y_{\delta \text{ rel } T}$	1.0	Common gear design is assumed.
Relative surface factor, $Y_{R \text{ rel } T}$	1.0	Static load case assumed.
Size factor, $Y_X$	1.0	Static load case assumed.

## A.2 Comparison for verification data

**Table A.2:** Comparison between transmission optimization tool output and MASTA.

Parameter	Optimization tool	MASTA
<i>Gear stage 1</i>		
Safety factor contact (static), $S_H$	1.133	1.192
Safety factor bending (static), $S_F$	1.267	1.270
Transverse contact ratio, $\varepsilon_\alpha$	1.545	1.545
Total contact ratio, $\varepsilon_\gamma$	3.832	3.832
Nominal tangential load, $F_t$	20.59 kN	20.59 kN
Nominal radial load, $F_r$	8.271 kN	8.271 kN
Nominal axial load, $F_a$	9.604 kN	9.604 kN
Gear mesh power loss	1.077 kW	0.986 kW
<i>Gear stage 2</i>		
Safety factor contact (static), $S_H$	1.029	1.092
Safety factor bending (static), $S_F$	1.0752	1.1047
Transverse contact ratio, $\varepsilon_\alpha$	1.5395	1.5395
Total contact ratio, $\varepsilon_\gamma$	2.8848	2.8848
Nominal tangential load, $F_t$	38.95 kN	38.95 kN
Nominal radial load, $F_r$	15.64 kN	15.64 kN
Nominal axial load, $F_a$	18.16 kN	18.16 kN
Gear mesh power loss	1.356 kW	1.347 kW
<i>Input shaft</i>		
Shaft safety factor	> 1	2.196
Bearing 1 safety factor, $s_0$	> 1	1.113
Bearing 2 safety factor, $s_0$	> 1	1.164
Bearing 1 power loss	0.1410 kW	0.1585 kW
Bearing 2 power loss	0.2402 kW	0.2409 kW
<i>Middle shaft</i>		
Shaft safety factor	> 1	1.782
Bearing 1 safety factor, $s_0$	> 1	1.221
Bearing 2 safety factor, $s_0$	> 1	1.889

**Table A.2:** (continued)

Influence factor	Optimization tool	MASTA
Bearing 1 power loss	0.2103 kW	0.2507 kW
Bearing 2 power loss	0.1492 kW	0.1767 kW
<i>Differential</i>		
Bearing 1 safety factor, $s_0$	> 1	1.752
Bearing 2 safety factor, $s_0$	> 1	1.473
Bearing 1 power loss	0.0961 kW	0.0768 kW
Bearing 2 power loss	0.0389 kW	0.0436 kW

### A.3 Visual evaluation of trends in population data

This section covers plots made for visual analysis linked with the results of model evaluation in Section 3.2.1.

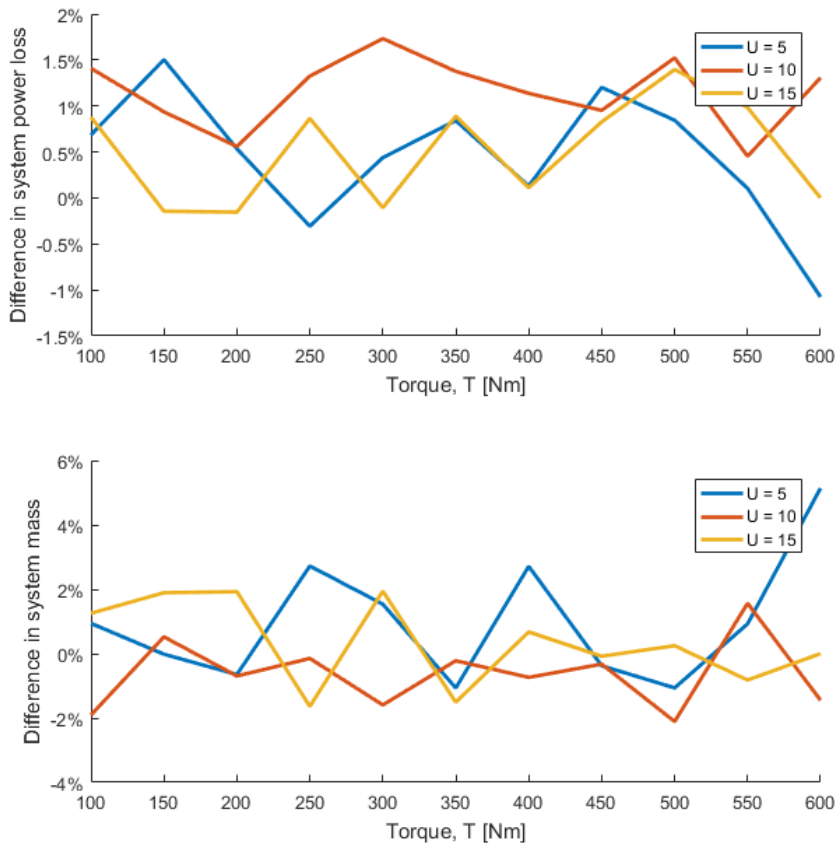


**Figure A.1:** Plots of sample data for visual analysis of trends depending on input torque. Shows the difference in system power loss (top) and system mass (bottom) depending on torque.

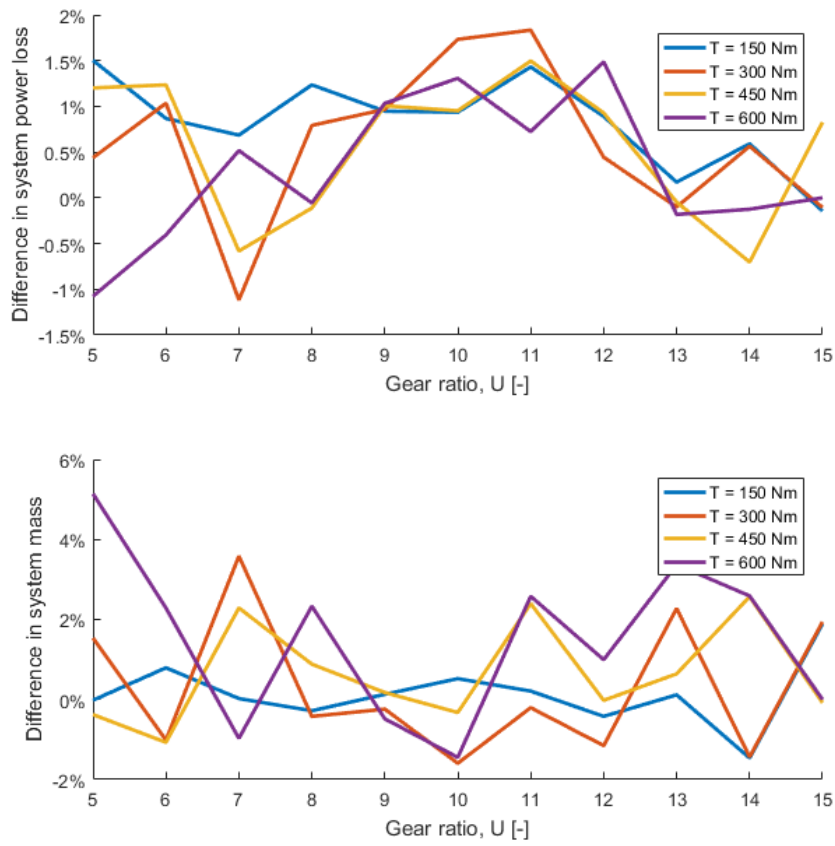


**Figure A.2:** Plots of sample data for visual analysis of trends depending on gear ratio. Shows the difference in system power loss (top) and system mass (bottom) depending on gear ratio.